AIR FORCE INSTITUTE OF TECHNOLOGY

AIR UNIVERSITY
UNITED STATES AIR FORCE

THRUST VECTORING WITH A PLUG NOZZLE

BY PLUG TRANSLATION

By

William J. Barnes, Jr. B.S.
1st Lt USAF

SCHOOL OF ENGINEERING

WRIGHT-PATTERSON AIR FORCE BASE

THRUST VECTORING WITH A PLUG NOZZLE

BY PLUG TRANSLATION

By

William J. Barnes, Jr. B.S.
1st Lt USAF

AF-WP-O-OCT 64 25

THRUST VECTORING WITH A PLUG NOZZLE BY PLUG TRANSLATION

THESIS

Presented to the Faculty of the School of Engineering of
the Air Force Institute of Technology
Air University
in Partial Fulfillment of the
Requirements for the Degree of
Master of Science

By
William Joseph Barnes, Jr. B.S.
1st Lt USAF
Graduate Astronautics

August 1964

Acknowledgements

I wish to express my appreciation to my thesis advisor, Lt G. A. Tsongas, for his able suggestions and kind support in the carrying out of this study. I also want to thank Mr. Frank Jarvis who, as my laboratory assistant, provided invaluable assistance. Lastly, I want to thank my wife who put in many hours in the preparation of this report.

William J. Barnes, Jr.

Contents

Page

List of Figures

List of Symbols and Subscripts

Symbols

A - Area, in^2

C_{Fp} - Plug axial thrust coefficient (see page 6)

dA_w - Element of plug wall area

F - Thrust, lb_f

g - Gravitational conversion factor, $32.174 \frac{ft\ lb_m}{lb_f\ sec^2}$

k - Ratio of specific heats

$\dot{m}$ - Mass flow rate, lb_m/sec

M - Mach number

P - Pressure, psia

R - Gas constant for air, $53.3 \frac{ft\ lb_f}{lb_m\ {}^{o}R}$

T - Temperature, ${}^{o}R$

V - Velocity, ft/sec

X/L - Ratio of axial distance along the plug to plug length

α - Angle between thrust vector and axial direction

β - Angle of nozzle lip to axial direction

ΔP_s - Pressure rise across oblique shock

θ - Local angle between plug wall and axial direction

Subscripts

a - Ambient conditions

B - Conditions in region of separation

t - Throat conditions

T - Transverse direction (see Fig. 2)

w - Conditions on plug wall

X - Axial direction (see Fig. 2)

o - Stagnation conditions

1 - Properties of Side 1 (see Fig. 2)

2 - Properties of Side 2, stepped side, (see Fig. 2)

Summary

A theoretical and experimental investigation was made of a convergent plug exhaust nozzle to determine if thrust vectoring could be achieved through the use of a translating plug which traveled in plane motion across a base region of slightly increased diameter. It was felt that thrust vectoring would be obtained by virtue of a pressure differential existing across the plug when the plug was translated from the centered position. Because certain two-dimensional aspects associated with the pressure differential existed, the study was reduced to the investigation of a two-dimensional convergent plug nozzle. The objectives were to determine the angle which the resultant thrust vector made with the axial direction when the plug was translated and, to determine the loss in axial plug wall thrust due to the step.

In order to determine the above-mentioned parameters the method of characteristics was applied to determine the theoretical pressure distribution over the plug wall contour of a basic Mach 2 plug nozzle with the plug in the fully translated position. To verify the above results the experimental study was made using a two-dimensional nozzle tested in cold flow. Two positions, the centered plug position and the position of maximum translation, were tested over the range of nozzle pressure ratios from the choked flow condition to near design pressure ratio of the nozzle. Flow visualization was accomplished by use of the Schlieren optical system.

Good qualitative correlation was obtained between the method of characteristics solution and experimental results. At a chosen value of nozzle pressure ratio of 6.15 the analytical solution predicted a

resultant thrust vector angle of not quite 4°. Experimental tests showed that the angle was nearer 2°. The results of the experimental investigation showed that the principle flow mechanism affecting thrust vectoring was a normal shock which moved axially down the plug with increasing pressure ratio. As a result of the presence of this shock along the plug neither significant nor consistent thrust vector angles could be obtained within the range of pressure ratios tested. There was an indication, however, that some measure of thrust vectoring might exist over a range of pressure ratios in the underexpanded regime. The axial thrust produced by the plug wall contour was materially reduced by the step which existed for the translated plug.

THRUST VECTORING WITH A PLUG NOZZLE BY PLUG TRANSLATION

I. Introduction

Background

A plug nozzle is characterized by having a central conical plug which controls the supersonic expansion of the exhaust jet. The plug is constructed to produce ideal isentropic expansion, with an axial velocity vector, at a particular value of the ratio of the total stagnation chamber pressure to the outside ambient pressure. For constant chamber pressure, this design nozzle pressure ratio may be defined by specifying a design altitude at which ideal expansion occurs. For most rocket nozzle applications this design altitude is usually a considerable distance above sea level. There are several variations of the basic plug nozzle configuration, but the only type considered here is that in which all supersonic expansion occurs downstream of the throat and external to any outer walls. This type is generally known as a convergent plug nozzle. The outer jet boundary is not confined within fixed geometry walls but, instead, is a free surface whose boundary is determined by the prevailing instantaneous nozzle pressure ratio. At low altitudes where the nozzle pressure ratio is below the design point, the free jet boundary is redirected by the ambient pressure and moves to produce an essentially axial exhaust velocity vector. Because of the movement of the jet boundary, compensation for overexpansion is provided and the nozzle performance, reflected by the thrust coefficient, tends

to remain constant up to the design altitude.

In contrast to the plug nozzle, the conventional convergent-divergent nozzle has a fixed geometry outer wall. Except when separation occurs, the wall expends the flow to a fixed pressure ratio defined by the ratio of the exit area to throat area. At pressure ratios below the design point, overexpansion occurs and the exit pressure is below ambient. A loss in thrust occurs because a portion of the internal wall has a pressure acting less than ambient. This portion produces a negative thrust which detracts from the overall nozzle thrust. The conventional nozzle, therefore, suffers reduced performance at low altitudes where the pressure ratio is below the design pressure ratio.

Because of the compensation provided by the ambient pressure to the convergent plug nozzle, the effects of overexpansion are reduced and performance exceeds that of the conventional nozzle at low altitudes (Ref 1). At higher altitudes where the pressure ratio is equal to or above the design value, the performance of the plug nozzle equals that of the conventional nozzle. One problem which has prevented the plug nozzle from being used in rocket vehicle applications is that of thrust vector control.

Thrust Vectoring

Thrust vectoring of present large rocket motors is often accomplished by gimballing the complete engine. A similar method of thrust vectoring is not practical for use with a plug nozzle. The maximum diameter of the plug nozzle lies in the plane of the throat and thus is directly adjacent to the aft end of the vehicle. This would severely complicate the attachment and gimballing mechanisms. Therefore, it is

desirable to use a method of thrust vectoring which does not require movement of the entire engine. Berman (Ref 2) suggests a method of thrust vector control which is obtained by gimballing the central plug alone, so that asymmetrical flow of the exhaust jet results. This method requires a somewhat complicated mechanical actuating system and also requires that the gimballed plug be supported against forces created by large pressure differentials when used for thrust vector control. There may also be performance reduction brought about by the variable throat area which results when the plug is gimballed.

Another method of thrust vectoring has been proposed which may reduce the stresses on the plug actuating mechanism and simplify the plug supporting system. With this method the entire plug is not movable, but instead, only that portion of the plug which extends downstream of the nozzle throat would be movable. The external plug would not be gimballed, but would move in two-dimensional translation across a plug base of slightly larger diameter (see Fig. 1). When the plug is in the centered position, an equal step or setback exists around the plug. As the plug is translated from the centered position, the step is decreased on one side and increased on the other. With decreasing step width, the plug contour approaches that of the ideal configuration. Losses created by flow separation will be reduced and the thrust will increase. For the side with increasing step, the plug contour retreats from that of ideal and is accompanied by a reduction in thrust. The net affect of plug translation should be a resultant pressure differential across the plug. It is expected that this pressure differential will be a function of plug translation and that maximum pressure differential will occur with the plug in the maximum translated position (maximum step on one

side - none on the other side). The side force or thrust component generated by the effect of the translated plug, if sufficient in magnitude and controllable, may provide thrust vector control for the nozzle.

Theoretical Model

The nature of the flow about a plug nozzle with a conical translating plug is definitely three-dimensional and an accurate analysis of the plug pressure distribution must reflect this fact. It appears, however, that the effect of plug translation is to produce a pressure differential across the plug which can be viewed in a somewhat two-dimensional manner. It must be admitted that the effects of cross-flow associated with the jet flow about a translating conical plug preclude a direct transition to two-dimensional analysis; but, by reducing the study to one in two dimensions, a much simpler approach, both analytical and experimental, may be taken while still retaining at least the basic mechanism of the thrust vectoring process.

Analytical Considerations

The forces acting on a plug nozzle may be determined by applying the momentum equation to the nozzle. Assuming constant properties along a straight sonic line at the throat, the thrust equation in vector form for the nozzle becomes

$$\vec{F} = \frac{\dot{m}\vec{V}_t}{g} + (P_t - P_a)A_t + \int (P_w - P_a)d\vec{A}_w \qquad (1)$$

The first two terms on the right hand side are positive and represent the jet thrust which acts on the nozzle at the throat. The third term is a summation of forces over the plug and represents a contribution to the total thrust due to the pressure distribution created by the

expanding exhaust jet. For a given pressure ratio the magnitude of this term is a function of the plug contour and in general may be either positive or negative. For a two-dimensional nozzle (see Fig. 2) the vector form of the thrust equation may be divided into two components - one axial and one transverse. The total axial thrust may be considered to be the sum of the axial thrusts for each side of the nozzle, and is given by

$$F_x = \frac{\dot{m}V_t}{g}\cos\beta + (P_t - P_a)A_t \cos\beta + \int (P_{w1} - P_a) \sin\theta_1 \, dA_{w1} \qquad (2)$$

$$+ \int (P_{w2} - P_a) \sin\theta_2 \, dA_{w2}$$

The net transverse force may be determined by taking the difference between the forces acting on each side of the nozzle. Since plug translation does not change the throat area of either side, it would be expected that the throat conditions would be the same for each side. Under this premise, the net transverse force acting on the nozzle reduces to merely the difference between the integrated plug transverse pressure distributions, and is given by

$$F_T = \int (P_{w1} - P_a) \cos\theta_1 \, dA_{w1} - \int (P_{w2} - P_a) \cos\theta_2 \, dA_{w1} \qquad (3)$$

The terms in Equation (2) not under the integral signs may be determined from measured conditions at the throat and known physical dimensions of the nozzle. Evaluation of the integrated terms in Equations (2) and (3), however, requires that the pressure be known at every point along the plug wall contour.

A measure of the thrust vectoring produced by the translated plug may be obtained by forming a ratio of the side force component to the axial force component. This ratio aids in defining the angle, α, which

is the angle the total thrust vector, $\vec{F}$, makes with the axial direction. Angle α would seem to be a function of the amount of plug translation and, to an undetermined degree, a function of the nozzle pressure ratio. Because of the step associated with the translated plug, ideal expansion past the plug will not occur; consequently, some undesired reduction in axial thrust must be accepted. A dimensionless thrust coefficient, C_{Fp}, may be defined to express the efficiency of the translated plug in producing axial thrust. The side of the plug which contains no step and, hence, conforms to the ideal contour will be taken as reference. The plug axial thrust coefficient, C_{Fp}, is defined as the plug axial thrust for the translated plug divided by the plug axial thrust for a plug which contains no step on either side. The thrust of the plug with no steps will be taken as twice the thrust of the ideal contour side mentioned above. Note that only the axial wall thrust components of the plug alone (the third and fourth terms of Equation (2))are used in this definition; the momentum and pressure thrust components (the first two terms of Equation (2)) which act at the nozzle throat are not included. At a particular nozzle pressure ratio, the momentum and pressure thrust components will be constant and only the thrust produced by the plug will vary with plug translation.

Objective

The objective of this study was to investigate the possibility of using the principle of the translating plug for thrust vector control of a convergent plug exhaust nozzle. A two-dimensional approach was taken with the result that Equations (2) and (3) could be used for the determination of the thrust vector angle, α, and the plug thrust

coefficient, C_{Fp}. For the determination of the individual terms of Equations (2) and (3) and for overall evaluation of the nozzle, a two phased program was utilized:

Theoretical Analysis. This phase consisted of the application of the method of characteristics to obtain analytically the pressure distribution along the translated plug. Subsequent use of Equations (2) and (3) enabled theoretical values of α and C_{Fp} to be determined for selected nozzle pressure ratios.

Experimental Investigation. To verify the theoretical analysis and experimentally investigate the problem, a two-dimensional model of a translating plug nozzle was built and tested in cold flow. Performance was evaluated by determining the plug contour pressure distribution through the use of appropriate pressure instrumentation. Results from both methods of study coupled with flow visualization by the Schlieren optical technique were used to identify the principle flow mechanisms existing within the translating plug nozzle.

II. Theoretical Analysis

The method of characteristics was applied to obtain the pressure distribution along the plug of a two-dimensional Mach 2 nozzle with translated plug. A detailed description of the experimental nozzle design and construction are presented in the section on apparatus. All theoretical solutions were obtained for the plug in the maximum translated position.

Method of Characteristics

The specific application of the general method of characteristics used in this analysis is described by Shapiro (Ref 3:462). This application is limited to two-dimensional, supersonic, irrotational, steady flow with the further assumption that the fluid is a perfect gas. Starting from a supersonic flow source of known properties, a semi-graphical solution for the downstream flow conditions may be obtained. Calculation proceeds by use of the "field method", wherein the stream properties of small regions or fields, bounded by Mach lines, are found for successive downstream positions. Appropriate equations are used to determine the flow properties and boundary lines of each individual field. The flow field is then plotted graphically.

Initial Conditions

The nozzle throat properties and the boundary conditions acting on the surface of the expanding jet must be specified in order to obtain a method of characteristics solution for the pressure distribution along the plug contour.

Throat Properties. Assuming a straight sonic line at the throat,

the throat pressure may be calculated from isentropic relations. The throat properties M_t and P_t comprise one set of initial conditions necessary for solution of the flow field.

Jet Boundary Conditions. For the ideal plug contour which exists on one side when the plug is in maximum translation, the flow follows the plug contour the complete length of the plug. The plug wall, whose direction is known at every point, defines one boundary of the expanding jet. The outer boundary of the expanding jet is a free surface of known constant ambient pressure. The throat properties together with the jet boundary conditions completely determine the flow field past the ideal plug contour.

For the side of the plug which contains the step or setback, an additional boundary condition must be specified. Because of the plug setback, the jet does not follow the contour of the plug but, instead, separates at the throat and impinges on the plug wall some distance down the plug. Thus, a bubble or region of separation is formed. The pressure in the separation bubble, P_B, is not generally known and its value may not be obtained from the method of characteristics solution. Chapman (Ref 4) investigated the problem of separation in supersonic flow with boundary layers of essentially constant pressure. It was concluded that the principle variable controlling pressure in regions of separation was the location of the transition from laminar to turbulent flow relative to the reattachment and separation positions. Because of the rapidly changing pressure downstream of the throat, the prediction of the pressure in the separated region of the plug nozzle appeared difficult from an analytical point and no further attempt at this was made. It had appeared at first, however, that some estimate

could be made of the bubble pressure from Coanda effect phenomena (Ref 5). In the Coanda effect, entrainment of surrounding fluid by a free jet near a wall causes a pressure differential across the jet and subsequent attachment of the jet to the wall. The pressure in the region of separation which is formed between the jet and the wall remains below ambient. Experimentally determined values of the bubble pressure (see Fig. 32) for the plug nozzle later showed that the Coanda effect was present but somewhat modified by the appearance of an oblique shock. To provide an adequate comparison to experimental results, an observed value of the bubble pressure was used to obtain a solution of the plug pressure distribution by the method of characteristics. To study the variation of the pressure distribution with bubble pressure a second solution was obtained assuming a somewhat smaller value for the pressure in the separated region.

Solution Procedures

Solution No. 1, $P_o/P_a = 6.15$. A solution for the pressure distribution of the translated plug was obtained for an assumed nozzle pressure ratio of 6.15. This pressure ratio was chosen to coincide with that of an experimental run so that comparisons could be made. The value of the bubble pressure used was the observed value $P_B = 18.65$ psia. A diagram of the graphical solution for the stepped side of the plug is shown in Fig. 3. This solution will be discussed first.

In Fig. 3 the dashed lines denote expansions waves while the solid lines within the jet boundary denote compression waves. The initial expansion of the jet occurs at the throat in the form of a series of centered expansion waves (called expansion fans). The directions of the

initial boundaries of the jet are determined by the ratio of the nozzle stagnation pressure to the outside pressures existing on each side of the jet. Thus, the expansion of the jet into the stepped region is not as great as that on the other side where expansion is to ambient pressure. The solution for the flow field begins by selecting a suitable number of expansion waves to represent the continuous expansion of flow which actually exists. These waves have the directions of the local Mach lines in the flow field. The more waves that are used the more accurate will be the solution. In this case four waves in the left expansion wave and five waves in the right expansion wave were assumed. As the waves cross each other quadrilateral fields are produced. Changes in flow properties occur as streamlines cross Mach lines bounding the fields.

At the point on the plug wall where the jet reattaches, a sudden change in flow direction defined by the local wall angle occurs. For the flow to negotiate the change in direction, an increase in pressure is required. This compression takes the form of an oblique shock wave which is propagated diagonally across the jet. The strength of the shock is a function of the upstream pressure and Mach number, and the turning angle required at the wall. In general the flow behind an oblique shock which interacts with continuous waves is no longer irrotational and the method of characteristics for isentropic flow may not be applied to a region where vorticity exists except as an approximation. However, this approximation often gives acceptable results, so the entropy changes which occur across the shock were ignored; i.e., the method of characteristics was applied without correction across the oblique shock. In view of the difficulty of applying a more exact solution, this was felt acceptable in this case.

Regions numbered A through E in Fig. 3 comprise the boundary of the jet adjacent to the wall. The pressures within the regions determine the pressure distribution on the plug contour. A plot of the resulting pressure distribution as a function of axial plug length is shown in Fig. 25. Since flow property changes occur in finite jumps across the fields, the graph is plotted in step fashion.

For the side of the plug reflecting the ideal contour, a very simple method may be used to obtain the pressure distribution. On this side the jet expansion may be represented by a continuous series of expansion waves centered at the plug lip. The flow follows the plug contour at every point and the turning of the flow is related to the local Mach number by the Prandtl-Meyer function (Ref 6:98). Since the direction of the wall is known at every point the Mach number of the jet at every point may be determined. From isentropic relations the pressure distribution past the plug may, thus, be obtained. Since the assumed nozzle pressure ratio is below the design pressure ratio of the plug contour (plug design pressure ratio = 7.8), overexpansion will occur. That is, at some downstream position the pressure will be expanded to ambient and further turning of the flow by the wall will result in compression of the jet (Ref 7:5). For higher nozzle pressure ratios this position occurs further downstream; and, at the design nozzle pressure ratio, ambient pressure is achieved at the end of the plug. The pressure distribution for the portion of the plug downstream of the point of minimum pressure may be obtained by use of the Prandtl-Meyer function with the consideration that compressive turning occurs. A graph of pressure as a function of plug axial length for the ideal contour side of the translated plug is shown in Fig. 25.

Solution No. 2, $P_o/P_a = 5.53$. A second solution for the pressure distribution past the translated plug was obtained for a pressure ratio lower than that which was used for the first solution. The exact value of 5.53 was chosen primarily because the computation was made easier. The assumed pressure in the region of separation on the setback side of the plug, in this instance, was not an experimental value but was chosen somewhat lower to determine the resulting effect on the total pressure distribution. The value of the pressure assumed was $P_B = 13$ psia. The same procedure as that used in the first solution was applied to obtain the pressures along the plug wall for both sides. The graphical solution for the stepped side is shown in Fig. 4 and a plot of the pressure distributions for both sides of the plug is presented in Fig. 26.

Summary of Theoretical Analysis

Observation of the pressure distribution curves for the setback side of the plug shows that the effect of reducing the pressure in the region of separation is to greatly increase the strength of the oblique shock which occurs when the jet impinges on the wall. The pressure rise across the oblique shock for the second solution ($P_o/P_a = 5.53$) is greater than that for the first solution ($P_o/P_a = 6.15$) even though the nozzle pressure ratio is less. This phenomena may be explained by the fact that for reduced P_B the initial jet boundary at the throat is inclined at a greater angle to the axial direction. (Compare 16.8^o for $P_B = 18.65$ psia to 22.3^o for $P_B = 13$ psia)- The jet thus impinges on the plug wall with a larger angle of incidence with the result that the flow must be turned through a greater angle.

The method of characteristics solutions for the stepped side of

the translated plug show that compression waves occur within the jet downstream of the initial expansion. Physically, they result from the fact that a free jet suddenly expanding to a lower pressure tends to overshoot and expand to a somewhat lower value. Compression waves occur to bring the pressure back up to that of the surroundings. The structure of the jet is characterized by a series of such expansions and compressions continuing downstream in periodic fashion until viscous effects dissipate the flow. A jet "wavelength" may be associated with the distance taken up by one cycle of expansion and compression. This wavelength, usually only considered for the initial cycle, varies directly with the nozzle pressure ratio. Due to the step existing on the setback side of the plug, the flow separates at the throat and the expansion is similar to that of a free jet. The method of characteristics solution for $P_o/P_a = 6.15$ shows that the expansion of flow past the plug bears a resemblance to the cyclic expansion of a two-dimensional free jet. In this case only the initial cycle appears. The wavelength appears to be somewhat longer than the plug and the compression waves coalesce just downstre of the plug end. The solution for $P_o/P_a = 5.53$ shows that the wavelength has decreased and compression waves impinge on the last portion of the plug wall. In Fig. 26 the pressure distribution curve indicates the increase in pressure due to the compression waves. It may be noticed that there is no cyclic expansion for the ideal contour side of the translated plug. This is because separation does not occur and the wall controls the expansion past the plug.

Experimental results in Ref 8:93 show that for axisymmetric jets with nozzle pressure ratios above approximately 3.8, the compression waves of the first wavelength coalesce and form a dish-shaped, normal

shock. For two-dimensional flow, Ref 9 includes characteristics calculations that show how the coalescence of the compression waves creates shocks within the jet. With increasing nozzle pressure ratio, the shocks grow in strength from intersecting shocks to strong normal shocks. The phenomena for two-dimensional jets occurs at a somewhat higher nozzle pressure ratio than for axisymmetric jets. While the method of characteristics calculations in this study do not show complete coalescence of the compression waves, it is believed that the similarity of the flow to that of a free jet warrants the expectance of a normal shock in actual flow conditions at sufficiently high nozzle pressure ratios.

By graphical integration of the plug pressure distribution, the differential side force and the axial forces acting on the translated plug contour were obtained for both method of characteristics solutions. Then, using the known throat dimensions and measured mass flow rate, Equations (2) and (3) were solved for the axial thrust and differential side force acting on the nozzle. The theoretical values of α and C_{Fp} were then determined. A summary of the results for the two solutions is presented below.

Solution No. 1, $P_o/P_a = 6.15$; $P_B = 18.65$ psia

$\alpha = 3.95^o$ $\qquad$ $C_{Fp} = 0.755$

Solution No. 2, $P_o/P_a = 5.53$; $P_B = 13$ psia

$\alpha = 2.55^o$ $\qquad$ $C_{Fp} = 0.713$

III. Experimental Investigation

Apparatus

The general laboratory arrangement of test equipment is shown in Fig. 5. Facilities of the Mechanical Engineering Laboratory of the Air Force Institute of Technology were used for the experiment. All apparatus was constructed by the school shops or was made available by the laboratory.

Model. Since this study was an initial investigation focused mainly on whether or not a significant side force could be developed across a translating plug, only two positions of the plug were tested. They were the centered plug position and the position of maximum translation. Initial considerations (see page 3) indicated that differential side force would be a function of plug translation and that the greatest pressure differential would occur with maximum translation. Thus, it was considered desirable to test this position first. Another advantage to be gained from testing this configuration is that an ideal plug contour exists on one side of the plug. This side may be used as a reference to determine the efficiency with which other plug contours, containing a setback, perform. The centered position of the plug was tested to determine the loss in axial thrust which occurs with this nozzle configuration also provided a position translated from that of the first so that it could be determined whether axial thrust was a function of plug translation.

To eliminate the need for a translation mechanism and facilitate pressure instrumentation, the plug and plug base were constructed as one unit. Simulation of plug translation was made possible by use of

two such plug-plug base combinations. The plug assembly shown within the test section in Fig. 6b simulates the plug in the maximum translated position. The other plug, shown outside the test section in the same photograph, corresponds to the plug in the centered position. The two plugs were constructed to be interchangeable within the test section.

The overall dimensions of the nozzle were restricted by the size of the test section windows and the available air supply. Throat dimensions of 1 inch by 0.191 inch for each side were chosen. Both plug contours downstream of the throat were identically designed by the method of characteristics (Ref 10) to give isentropic Prandtl-Meyer expansion about a lip at a pressure ratio of 7.8. At this pressure ratio the exit jet flows at Mach 2 past the plug apex. The design pressure ratio of 7.8 was chosen primarily from initial estimates of the available air supply (this value later proved to be optimistically high as the maximum pressure ratio obtained was approximately 6.5). The accommodation of necessary pressure taps within the plug body prevented the use of a spiked end plug for the tests. The plug wall contours were held fixed and a widening section was built into the plug to increase the width. This created a base region on the end. Although a pressure tap was installed to measure the base pressure, the contribution of the base to the axial thrust was later found to be negligible and was not included as a part of the plug axial thrust.

A somewhat arbitrary step of 7/16 inch was chosen for the translated plug. In specifying this dimension, a trade-off was made between the increase in thrust vectoring and the decrease in axial thrust which would probably occur with increases in step width. Large setbacks would obviously be impractical. Once the step for the translated plug was

chosen, the step for the centered plug became 7/32 inch for each side.

The nozzle components consisting of two plugs and one set of nozzle lips were cut from 1/4 inch brass stock and machined to a thickness of 0.191 inch. Ordinary white bond paper was used for gasket material between the nozzle components and the test section with the result that the final thickness was increased to 0.199 inch. Pertinent final dimensions are given below; other dimensions are given in Fig. 34.

Throat width each side	= 1.000 inch
Plug thickness	= 0.199 inch
Throat area each side $(\frac{A_t}{2})$	= 0.199 in^2
Nozzle lip angle (β)	= 26.4°

To accommodate the tubing for measuring the plug wall pressures, a cavity was milled into one side of the plugs. After the tubing was installed, the cavity was filled with a non-shrinking plastic, and sanded smooth. The centered plug with all taps in place, before being filled, is shown in Fig. 6b.

The test section, which housed the nozzle assembly, consisted of a base plate, two side plates, and glass restraining rings. These components were constructed of aluminum plate with dimensions as given. Standard quality Schlieren glass provided in the laboratory was used for sidewall windows. All nut and bolt hardware used were standard items.

Air Supply. Two compressors, each rated at approximately 100 psi gage, provided dry oil-free air for the experiment. The compressors, connected in parallel, supplied air to the vertical settling chamber shown beneath the test section in Fig. 6a. Nozzle total pressure was regulated by use of a hand-opperated valve. Steady flow at a particular pressure ratio was maintained by use of a bleed valve located upstream

of the flow meter. The bleed valve kept both compressors operating at all times and prevented pump cycling. At the highest obtainable pressure ratios the flow rate from the compressor tanks was greater than compressor capacity and steady flow could not be maintained long enough for all pressure data to be recorded. Nevertheless, almost steady flow conditions were obtained by making simultaneous readings of all pressure indicating instruments. A Graphex camera with a Polaroid film holder was used to make photographs of the readings. These were then read with the aid of a low power microscope.

Instrumentation. The static pressures along the plug wall downstream of the throat were measured with two banks of nine each, 30 inch mercury U-tube manometers. Nozzle lip pressures and plug throat pressures were measured with five 0-100 inch mercury manometers. Nozzle stagnation pressure was measured at the vertical settling chamber by a 0-200 inch mercury dial gage graduated in 0.2 inch increments.

The flow-meter consisted of a 1.05 inch diameter flat plate orifice placed in the two inch diameter air supply line. Flange pressure taps were used to determine the pressure drop across the orifice and the pressure drop was measured by a 0-100 inch mercury U-tube manometer. Pressure upstream of the orifice was measured with a 0-200 inch mercury dial gage graduated in 2 inch increments. The flow-meter installation conformed to the standards of the ASME (Ref 11).

Temperature upstream of the flow meter was measured with a copper-constantan thermocouple placed just upstream of the orifice. Nozzle stagnation temperature was assumed to be approximated by the temperature upstream of the flow meter; hence, its value was determined at the same location.

Schlieren Optical Equipment. A Schlieren optical system was used to observe the nozzle flow. Photographs were taken with a bellows type camera having a Polaroid film holder. All photographs were made with the knife edge horizontal. Polariod type 42 film was used throughout.

Test Program

Both the translated and centered plug configurations were tested over a range of pressure ratios of approximately 2.5 to 6.5. Data was recorded at chamber pressure (P_o) intervals of 10 inch Hg for the translated plug and intervals of 20 inch Hg for the centered plug, from 190 inch Hg absolute down to ambient.

Run Procedure. A typical data run for all but the highest nozzle pressure ratios was initiated by obtaining steady flow at the desired chamber pressure. This was accomplished by carefully adjusting the line flow and bleed valve to attain proper balance of flow to the settling chamber. Manometer readings of the pressures at the nozzle throat and on the plug contour were recorded. The pressure upstream of the flow-meter and the pressure drop across the orifice were also recorded. The temperature upstream of the flow-meter, which was also taken for the nozzle stagnation temperature, was determined from a potentiometer reading.

At the highest pressure ratios (above $P_o/P_a = 6$), the run procedure differed somewhat in that the bleed valve was not used. Instead, the line flow valve was fully opened quickly. The pressure in the settling chamber rose to a maximum value, and then fell slowly as the pressure in the compressor tanks dropped. When the desired chamber pressure (indicated by the chamber pressure gage) was reached, a photograph was

taken of the pressure readings.

Test Conditions. To assure that the air flow was divided equally between the two nozzle halves and that mass flow rate was the same for both plug configurations, the throat dimensions were controlled to within 0.001 inch. This later afforded the assumption, for computation purposes, that equal mass flow was achieved even though some small deviations in throat pressure were observed. There was some initial concern about the possibility of pressure leakage occurring across the plug between the glass windows and the plug face. While no adequate means was found to measure such leakage, it was thought to be largely eliminated by the use of a rubber cement sealant which provided a good bond to both the glass and the paper gasket material.

Run Reproducibility. A hysteresis effect, associated with recorded wall pressure measurements, was observed. This was believed to be largely due to lag in the pressure lines or, to some extent, instrument effects. To eliminate this, runs were made by approaching the desired pressure ratio from above and below. An average was taken between the two sets of data. By following this procedure, pressure readings were reproducible to within 0.5 inch Hg.

Schlieren Photographs. Schlieren photographs of the flow on both sides of the plug were taken for each run. These are presented in Figs. 19 through 24. To obtain large scale photographs, it was necessary to take pictures of each plug side separately. Therefore, the photographs shown are composites made from two pictures taken at the same value of chamber pressure. Because it was necessary to move the Schlieren apparatus each time, some misalignment may be noticed.

Data Reduction

Mass Flow Rate. The nozzle mass flow rate, $\dot{m}$, was calculated from recorded flow-meter data using the standard ASME equations found in Ref 10. The symbols used were taken directly from Ref 10 and are as defined below. They are unique to this calculation and should not be confused with possibly similar symbols used elsewhere in this report. The basic equation for the mass flow rate is

$$\dot{m} = 0.525\ K\ Y_1\ D_2^2\ \sqrt{\rho_1 \Delta P} \tag{4}$$

where

ρ_1 = Density upstream of orifice, lb_m/ft^3

ΔP = Pressure drop across orifice, psi

D_1 = Pipe diameter, 2 inch nominal

D_2 = Orifice diameter, 1.050 inch

D_2/D_1 = Diameter ratio, 0.525

K = Flow coefficient, function of Reynolds number, R_d, and diameter ratio D_2/D_1 (Ref 10:111)

k = Ratio of specific heats, 1.4

$$Y_1 = 1 - [0.41 + 0.35\ (D_2/D_1)^4]\ \frac{\Delta P}{P_1 k}$$

The Reynolds number based on the orifice diameter is defined by

$$R_d = \frac{48\ \dot{m}}{D_2\ \pi\ \mu_1} \tag{5}$$

where

μ_1 = Upstream dynamic viscosity, $lb_m/sec\ ft$

The calculation of the mass flow rate proceeds by assuming a value of Reynolds number, R_d, and finding the corresponding value of K.

Equation (4) is then solved for the mass flow rate. Using the calculated value of mass flow, the Reynolds number is found from Equation (5). If the calculated and assumed values agree, then the flow rate is determined. If the R_d values are not the same, a new value is assumed and iteration proceeds until agreement is made. A judicious first assumption usually results in only one iteration having to be made. A graph showing mass flow rate as a function of nozzle pressure ratio is given in Fig. 29.

Axial Thrust Calculations. The nozzle axial thrust, F_x, was determined by use of Equation (2).

$$F_x = \frac{\dot{m}V_t}{g}\cos\beta + (P_t - P_a)A_t\cos\beta + \int (P_{w1} - P_a)\sin\theta_1\, dA_{w1} + \int (P_{w2} - P_a)\sin\theta_2\, dA_{w2} \qquad (2)$$

By use of isentropic relations the throat velocity may be expressed in the form

$$V_t = \frac{\dot{m}R}{A_t}\frac{T_o}{P_o}\left(\frac{P_o}{P_t}\right)^{1/k} \qquad (6)$$

The insertion of Equation (6) into Equation (2) gives the equation in the form for computation

$$F_x = \frac{\dot{m}^2 R}{gA_t}\frac{T_o}{P_o}\left(\frac{P_o}{P_t}\right)^{1/k} + (P_t - P_a)A_t\cos\beta + \int (P_{w1} - P_a)\sin\theta_1\, dA_{w1} + \int (P_{w2} - P_a)\sin\theta_2\, dA_{w2} \qquad (7)$$

The measured values of $\dot{m}$, P_o, and P_t were used, together with the known value of A_t and β to evaluate the non-integrated terms of Equation (7). The value of P_t used was obtained by averaging the throat pressure measurements. The axial plug force for each side was obtained by graphical integration of plots giving pressure as a function of wall height (distance from nozzle centerline). The curves were mechanically

integrated with a polar planimeter. The axial force produced by the step was included in the integrations but, as noted previously, the force produced by the plug end was not.

Transverse Force Calculation. Since the throat areas on each side of the nozzle were the same, equal mass flow was assumed. The small variations in throat pressures between the two sides were ignored and the transverse force was taken to be the difference between the integrated plug wall pressure distributions. The transverse force is thus given by Equation (3).

$$F_T = \int (P_{w1}-P_a) \cos\theta_1 \, dA_{p1} - \int (P_{w2}-P_a) \cos\theta_2 \, dA_{p2} \qquad (3)$$

Curves giving plug wall pressure as a function of plug axial length were plotted (see Figs. 7 through 18) and mechanically integrated. Note that, as given here, the direction of transverse force has been assumed as shown in Fig. 2. Consequently, a negative sign (see Fig. 30) indicates transverse force in the opposite direction.

The total nozzle thrust ($\vec{F}$) is obtained from the vector sum of the axial and transverse components of thrust. A plot showing the variation of $\vec{F}$ with nozzle pressure ratio is given in Fig. 33.

Determination of Angle α. Angle α is defined as the angle the thrust vector makes with the axial direction. Therefore, α may be found from

$$\alpha = \tan^{-1} \frac{F_T}{F_A} \qquad (8)$$

For the translated plug a curve giving α as a function of nozzle pressure ratio is shown in Fig. 30.

Determination of C_{Fp}. For each pressure ratio, the plug axial

thrust for the ideal side of the translated plug was used as the reference value. A numerical example best illustrates how C_{Fp} was found.

For the translated plug at $P_o/P_t = 3.4$

Plug axial force on ideal side = 0.921 lb_f

Plug axial force on setback side = 0.638 lb_f

$$C_{Fp} = \frac{0.921 + 0.638}{2(0.921)} = 0.846$$

For the centered plug at $P_o/P_a = 3.4$

Plug axial force on left side = 0.675 lb_f

Plug axial force on right side = 0.441 lb_f

$$C_{Fp} = \frac{0.675 + 0.441}{2(0.921)} = 0.606$$

Note that the plug axial force on the ideal contour side (0.921 lb_f) was the thrust produced by a side with no step. By doubling this value the total axial force of a plug with no step on either side is obtained. Such a plug configuration would produce the ideal or maximum value of thrust. It may be noticed that the forces for the centered plug were not the same on each side of the plug. This was due to differences in the pressure distributions. A curve giving C_{Fp} as a function of nozzle pressure ratio for both the translated and centered plugs is shown in Fig. 31.

Experimental Findings

The following observations of the experimental data were made. A more complete discussion together with comparisons to the theoretical analysis is given in the section on results.

Nozzle Lip Pressures. Two pressure taps, one on the lip and one on the plug body, were used to measure the throat pressure for each side of the nozzle. The observed throat pressure measured at the nozzle lip was approximately 5% above that of the theoretical throat pressure (based on theoretical Mach 1 flow at the throat for the observed chamber pressure P_o), at all pressure ratios. The throat pressure measured on the plug body, however, remained consistently approximately 17% below theoretical. This phenomena was probably due to premature supersonic expansion of the flow around the upstream plug body (Ref 7:5). Thus, a curved sonic line existed in the throat region. This effect is illustrated graphically by the wall pressure distribution curves for the ideal contour side of the translated plug (see Figs. 7 through 12); comparisons with similar curves in Ref 7 showed a close correlation. Because a straight sonic line does not exist at the throat, the thrust equation (Equation (1) applied to the nozzle is not completely valid and a more general form would be needed for exact analysis. Because of the difficulties involved with determining the actual throat pressure distribution, Equation (1) was applied using an average value for the throat pressure. The lip and plug body pressures on each side were averaged and compared. For all pressure ratios tested, the averages were within 0.3 inch Hg of agreement. This was thought to be within experimental error. A single value of P_t for use in Equation (1) was obtained by taking the mean between the average values of each side.

Pressure Distribution for Setback Side of the Translated Plug Configuration. The plug wall pressure curves for the setback side show three significant features. The first is the region of approximately constant low pressure existing on that portion of the wall where the

flow is separated. The second feature is the steep pressure rise which occurs when the flow reattaches to the wall. The third feature is another pressure rise which occurs at a point further down the wall. Observations of the Schlieren photographs (Figs. 19 through 21) show that the first pressure rise is due to an oblique shock wave which is initiated at the jet attachment point and continues diagonally across the jet. The second pressure rise is caused by a normal shock wave which moves downstream with increasing pressure ratio.

Pressure Distribution for Centered Plug. The plug wall pressure curves presented in Figs. 13 through 18 show that there were some differences in pressure distribution between the two sides of the centered plug. This occurred even though the throat pressures for both sides were found to be within 0.3 inch Hg of agreement for all pressure ratios tested. No conclusive explanation of this effect can be offered. There may have been undetectable variations in the pressure tap angles on opposite sides. If the angles were not identically the same, different values of wall pressure would be recorded.

The general shape of the wall pressure distribution curves for the centered plug were similar to those of the setback side of the translated plug. Both the oblique and normal shock waves were present. The normal shock behaved similarly in that it moved downstream with increasing nozzle pressure ratio.

IV. Results and Comparisons

Comparison Between Theoretical Analysis and Experimental Investigation

A comparison of pressure distribution curves for the pressure ratio of 6.15 shows that for the ideal contour side of the translated plug, the observed wall pressures agree closely with those of the theoretical expansion (see Fig. 28). The only significant difference between the curves occurs at the throat region where, because of premature supersonic expansion, the experimental pressure distribution was lower than theoretical.

For the setback side of the translated plug the pressure distribution predicted by the method of characteristics approximates in step fashion the experimental distribution. The experimental results confirmed the oblique shock which originated at the jet attachment point. The pressure rise due to the oblique shock was closely predicted by the analytical method for $P_o/P_a = 6.15$ using the observed value of P_B (see Fig. 27). The primary difference between the two curves in Fig. 27 was the pressure rise near the end of the plug obtained from experiment. The Schlieren photograph in Fig. 21a shows that the pressure rise was due to a normal shock wave. The normal shock, which was not predicted analytically, but whose existence was suspected, was observed at all values of nozzle pressure ratio above approximately 3.4. Previous discussion indicated that normal shocks should have occurred at pressure ratios somewhat above 3.8 (this was the value for an axisymmetric nozzle). Thus, the normal shock occurred at pressure ratios slightly less than would normally have been expected. There are two possible explanations for this phenomena. The first is that there may have been boundary

layer effects present on the test section windows which precipitated the normal shock at the lower pressure ratios (below 3.8). Because of the small thickness of the nozzle (0.199 inch), there had been some concern initially whether two-dimensional flow could be achieved with the test apparatus. Comparison of the pressure distributions in Fig. 28 shows, however, that the experimental pressure distribution for the ideal contour side is very close to the theoretical expansion. Therefore, it is believed that any sidewall effects were relatively minor and that two-dimensional flow throughout the nozzle was essentially obtained. The second possible cause for the premature appearance of the normal shock may have been the oblique shock which extended diagonally across the jet. The pressure rise due to this shock may have disrupted the downstream flow and aided in the formation of the normal shock. In all probability a combination of both of the above effects was responsible for the early appearance of the normal shock. The overall experimental results indicate that test conditions were adequate. The premature occurrance of the normal shock did not appear to have a significant effect on the performance evaluation of the translating plug nozzle.

The values of α and C_{Fp} calculated from analytical and experimental data for the nozzle pressure ratio of 6.15 are presented below for comparison purposes.

Method of Characteristics Solution, $P_o/P_a = 6.15$

$\alpha = 3.95^o$ $\qquad$ $C_{Fp} = 0.757$

Experimental Data, $P_o/P_a = 6.15$

$\alpha = 1.72^o$ $\qquad$ $C_{Fp} = 0.823$

The value of C_{Fp} predicted by the method of characteristics was in fairly good agreement with the experimental value. This was expected since the experimental value of P_B was used in the analytical solution, and as explained previously the pressure in the region of separation has a large effect on the plug axial thrust. The value of α predicted analytically was less than the experimental value. This was because the analytical pressure distribution plotted as a function of plug axial length was lower than the observed pressure distribution (see Fig. 27). If more waves had been used in the analytical solution a closer correlation to the experimental data would probably have resulted. The significant difference between the curves was that for the pressure ratio of 6.15, the method of characteristics did not predict the pressure rise due to the normal shock. Another difference existed at the throat region where, because of a pressure leak-back from the downstream flow, there was an increase in pressure within the region of separation near the jet attachment point.

Variations of Pressure in Separation Region With Pressure Ratio

For the setback side of the translated plug at pressure ratios from approximately three to four, P_B decreases for increasing pressure ratio. This phenomena is probably due to the Coanda effect. Fluid is entrained by the jet between the separation and reattachment points. At reattachment, some fluid is turned and forced back into the separation region to satisfy continuity requirements. A vortex of reduced pressure is created. At a pressure ratio of approximately 4.5, the pressure in the separation region starts, unexpectedly, to rise. An explanation of this effect is as follows. At a pressure ratio of between four and five, the oblique

shock (see Fig. 19b and 20a) is formed at the reattachment point. The strength of the shock is a function of the upstream conditions and increases for increasing pressure ratios. As the shock strength increases, the fluid boundary layer next to the wall is unable to withstand the accompanying pressure rise. There occurs leakage of pressure back into the separation region. The pressure, P_B, thus, starts to increase. The variation in P_B as a function of pressure ratio is shown in Fig. 32. On the same graph there is also a plot of the pressure which exists just downstream of the oblique shock. The difference between the two curves, therefore, is a measure of the pressure rise across the shock. This pressure rise appears to remain constant for increasing pressure ratios. Thus, there appears to be an almost constant pressure differential which the boundary layer can sustain. While a curve was not plotted for the separation pressure of the centered plug, observation of the pressure distribution curves shows that the behavior of P_B is similar to that of the translated plug. In this case, though, the minimum occurred at a nozzle pressure ratio of approximately 3.4 while for the fully translated plug it occurred at approximately 4.09. Because of the increase of P_B which occurs for an increase in pressure ratio, the value of the plug thrust coefficient changes somewhat.

Variations of C_{Fp} With Pressure Ratio

The influence of the pressure in the separation region on the plug C_{Fp} is shown by the similarity between the curves given in Figs. 31 and 32. This similarity is due to the fact that axial plug thrust is directly related to the sine of the local wall angle. Since the local wall angle is greatest at the throat, these portions contribute most

heavily to the axial thrust.

The curves of C_{Fp} as a function of pressure ratio for the translated and centered plugs show that above a pressure ratio of approximately 4.5 the plug thrust coefficients are almost equal. This indicates that C_{Fp} is not a function of plug translation above that limiting pressure ratio.

Analysis of Thrust Vectoring Mechanism

The thrust vector angle, α, seemed to be most strongly influenced by the normal shock. This is shown in Fig. 30 which indicates the variation of α with pressure ratio. As the normal shock moved down the plug with increasing pressure ratio, it caused α to first decrease to a negative value and then increase as the shock moved past the end of the plug. The thrust vector angle appears to be increasing at the highest pressure ratios tested. There is reason to believe that this trend would continue at higher pressure ratios since the normal shock would move farther downstream. In this study a plug nozzle with design pressure ratio of $P_o/P_a = 7.8$ was tested at pressure ratios up to $P_o/P_a = 6.5$. Thus, the range of pressure ratios for which significant thrust vectoring may be achieved appears to extend into the underexpanded flow regime. Since, as indicated in the background discussion, the convergent plug nozzle has greatest utility when operated in the overexpanded regime, there does not seem to be any immediate advantage to this method of thrust vectoring if such thrust vectoring can be obtained only during underexpanded operation.

This study was initiated primarily to investigate the use of a conical convergent plug nozzle with translating plug. It is believed

that the results of this two-dimensional study are applicable to such a nozzle in that the basic thrust vectoring process is similar. With a conical nozzle any pressure differential existing across the plug is subject to mitigating effects by cross flow. Thus, the two-dimensional nozzle for which the jets on opposite sides are completely separated probably represents the maximum thrust vectoring which could be obtained through the use of the translating plug principle. The thrust vectoring obtained for the conical nozzle would then be somewhat less than that obtained from the two-dimensional nozzle. Based on this investigation the exact amount of thrust vectoring which would be obtained by a conical nozzle cannot be determined. Such a determination would have to be made from actual testing.

V. Conclusions

Comparisons between the analytical investigation and the experimental results verified the method of characteristics as an effective means for analyzing the two-dimensional expansion of flow past the plug wall contour. Good qualitative correlation between the two methods was obtained. Quantitative results for the chosen pressure ratio of P_o/P_a = 6.5 showed that the method of characteristics was more optimistic in predicting the thrust vectoring which could be obtained with the plug in the maximum translated position. The analytical value was $\alpha = 3.95^\circ$, while the experimental value was $\alpha = 1.72^\circ$.

As a result of the experimental investigation the following conclusions concerning the test parameters were reached.

1) The thrust vector angle α, was controlled mostly by a normal shock which originated and moved downstream along the wall contour of the setback side of the translated plug.
2) Angle α was a function of nozzle pressure ratio and varied from -1.5° to $+2.5^\circ$ over the range of pressure ratios tested. At the highest pressure ratio tested, the value for the thrust vector angle was $\alpha = 2.5$ and, was increasing with pressure ratio.
3) The step produced a sizable reduction in the axial thrust contribution of the plug wall contour. The larger step existing for the fully translated plug caused a greater reduction than the half step of the centered plug.
4) The plug axial thrust coefficient, C_{F_p}, was found not to

be a function of plug translation above a nozzle pressure ratio of 4.5, i.e., the total axial wall contour thrust (both sides) was approximately the same above $P_o/P_a = 4.5$ for both the centered and the translated plug configurations. The average value of C_{F_p} for the two plug configurations increased from 0.74 at $P_o/P_a = 4.5$ to 0.83 at $P_o/P_a = 6.15$.

Based on the results of this investigation, neither significant nor consistent thrust vectoring could be achieved over the range of pressure ratios tested. The thrust vector angle, α, varied from positive values at low pressure ratios, to negative values at intermediate pressure ratios, to increasingly positive values at the highest pressure ratios tested. There is reason to believe, however, that at least for a certain range of pressure ratios the upward trend will continue and that significant thrust vectoring may be obtained for pressure ratios higher than those investigated in this study.

VI. Recommendations

In order to provide correlation to the present study and to determine the actual thrust vectoring which would be obtained from a conical plug nozzle with translating plug, it is recommended that a three-dimensional model be built and tested (for instance see Fig. 1). The range of operation should be extended to include nozzle pressure ratios in the underexpanded regime. It would be advantageous to test the nozzle in hot flow. This would provide an opportunity to determine the effect of the step on heat transfer phenomena.

Bibliography

1. Ciepluch, C.C., G.H. Krull, and F.W. Steffen. Preliminary Investigation of Performance of Variable-Throat Extended-Plug-Type Nozzles Over Wide Range of Nozzle Pressure Ratios. RM E53J28. Washington D.C., NACA, 1954.

2. Berman, K., and F.W. Crimp, Jr. Performance of Plug-Type Rocket Exhaust Nozzles. Presented at the American Rocket Society Solid Propellant Rocket Research Conference, Princeton, N.J. January 28-29, 1960. ARS Preprint No. 1047-60.

3. Shapiro, A.H. The Dynamics and Thermodynamics of Compressible Fluid Flow, Vol I, The Ronald Press Company, New York, 1953.

4. Chapman, D.R., D.M. Kuehn, and H.K. Larson. Investigation of Separated Flows in Supersonic and Subsonic Streams with Emphasis on the Effect of Transition. TN 3869. Washington D.C., NACA, 1957.

5. Elsby, C.N. Jet Switching Phenomena in a Choked Flow Coanda-Effect Nozzle. Thesis, Air Force Institute of Technology: Wright-Patterson AFB, Ohio, August 1963.

6. Liepmann, H.W., and A. Roshko. Elements of Gas Dynamics, John Wiley & Sons, New York, 1962.

7. Beale, W.T., and J.H. Povolny. Internal Performance of Two-Dimensional Wedge Exhaust Nozzles. RM E56K29b. Washington D.C., NACA, 1957.

8. Love, E.S., and C.E. Grigsby. Some Studies of Axisymmetric Free Jets Exhausting From Sonic and Supersonic Nozzles Into Still Air and Into Supersonic Streams. RM L54L31. Washington D.C., NACA, 1955.

9. Pack, D.C. "On the Formation of Shock Waves in Supersonic Gas Jets (Two-Dimensional Flow)." Quarterly Journal of Mechanics and Applied Mathematics, Vol I, Part 1: 1-17 (March 1948).

10. Conners, J.F., and R.C. Meyer. Design Criteria for Axisymmetric and Two-Dimensional Supersonic Inlets and Exits. TN 3589. Washington D.C., NACA, 1956.

11. A.S.M.E. Special Research Committee on Fluid Meters. Fluid Meters Their Theory and Application, Part I. New York: America Society of Mechanical Engineers, 1937.

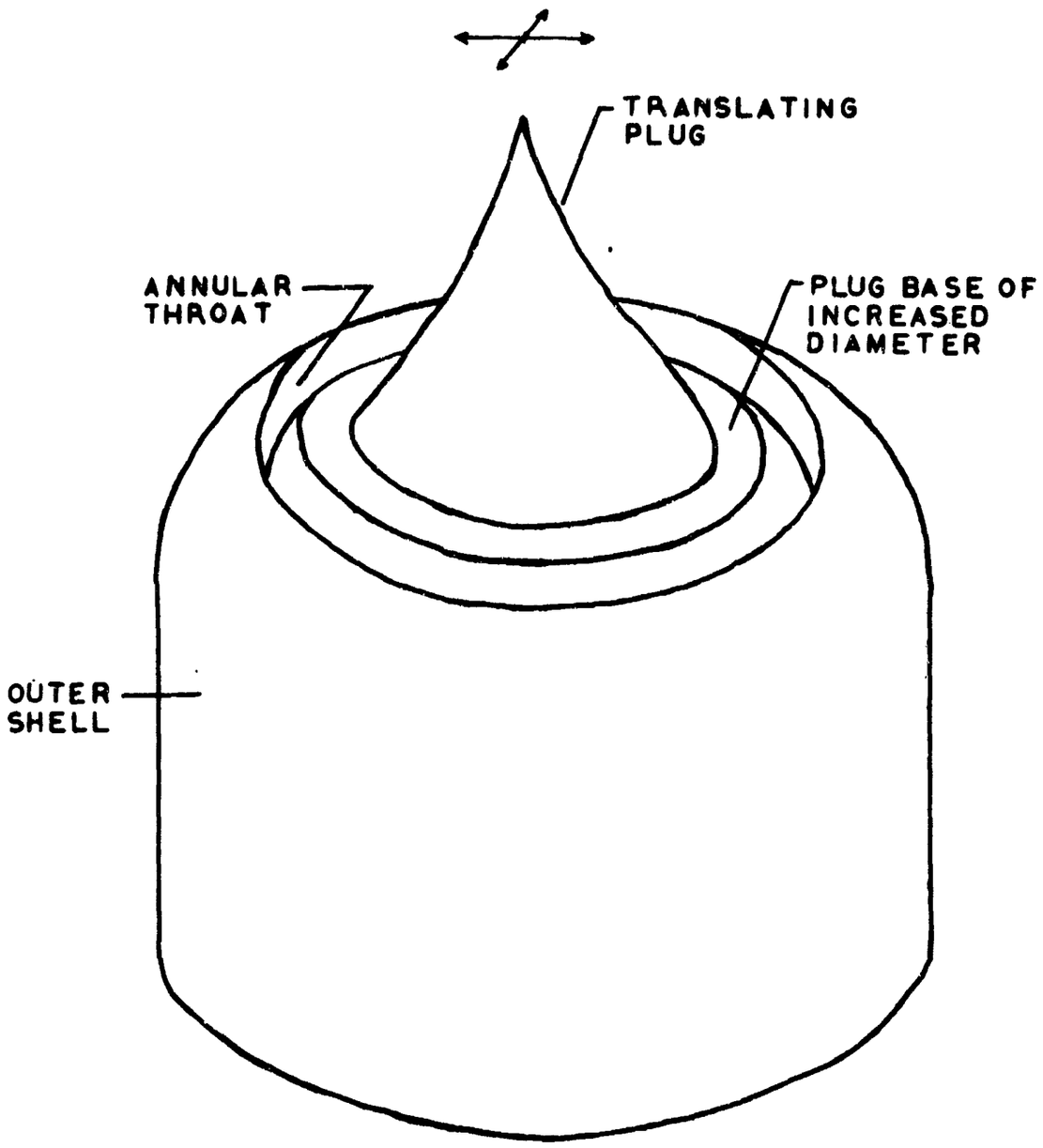

Fig. 1

Sketch of Proposed Convergent Plug Nozzle
With Translating Plug

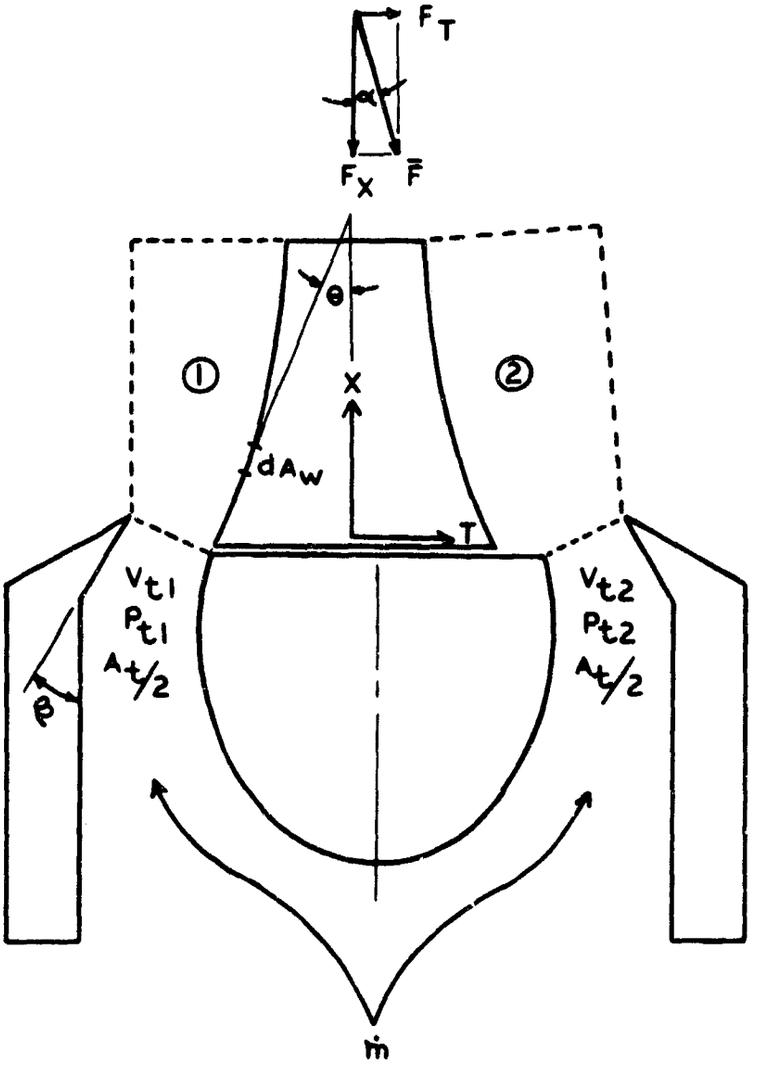

Fig. 2

Two-Dimensional Plug Nozzle
With Translating Plug

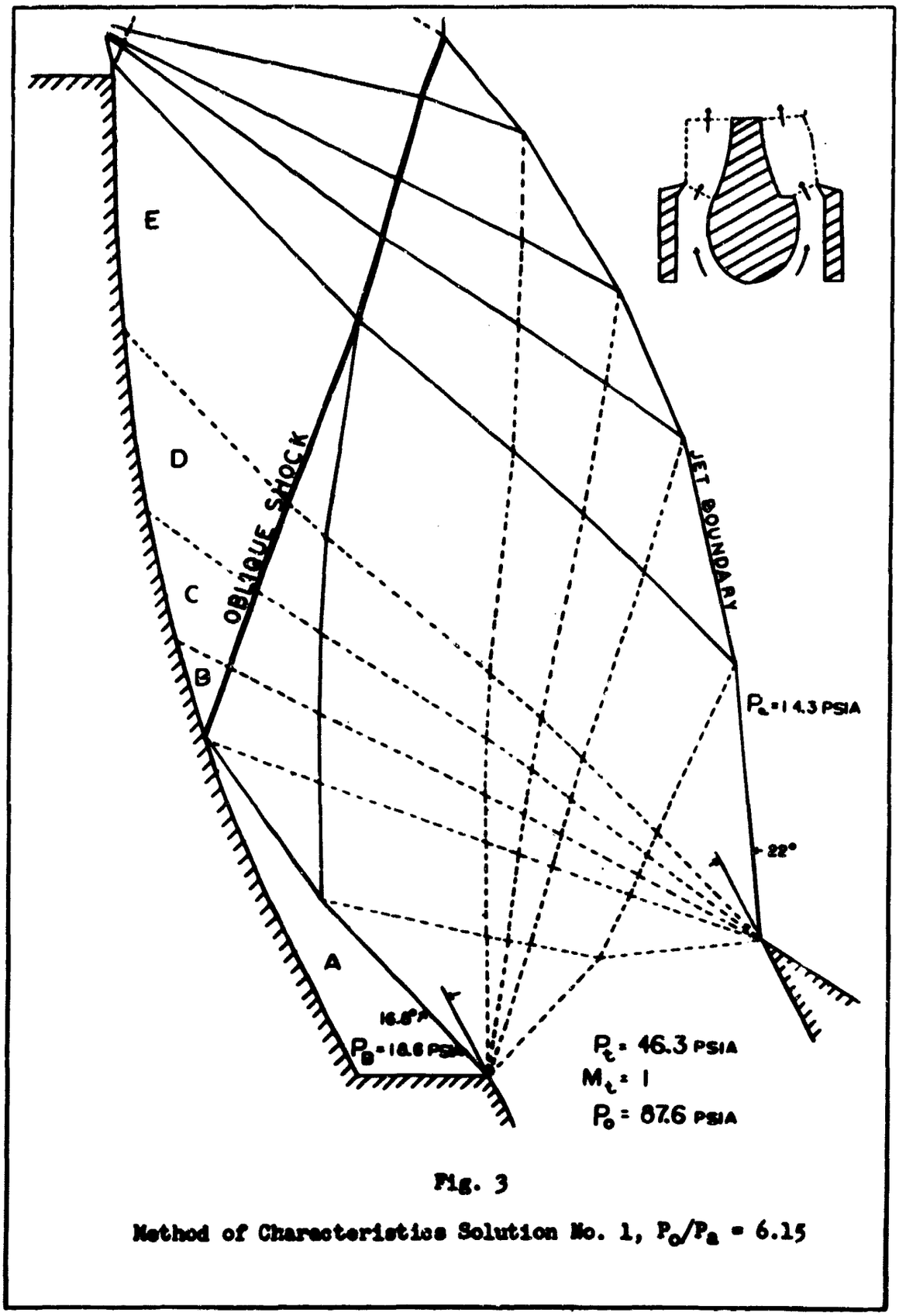

Fig. 3

Method of Characteristics Solution No. 1, P_o/P_a = 6.15

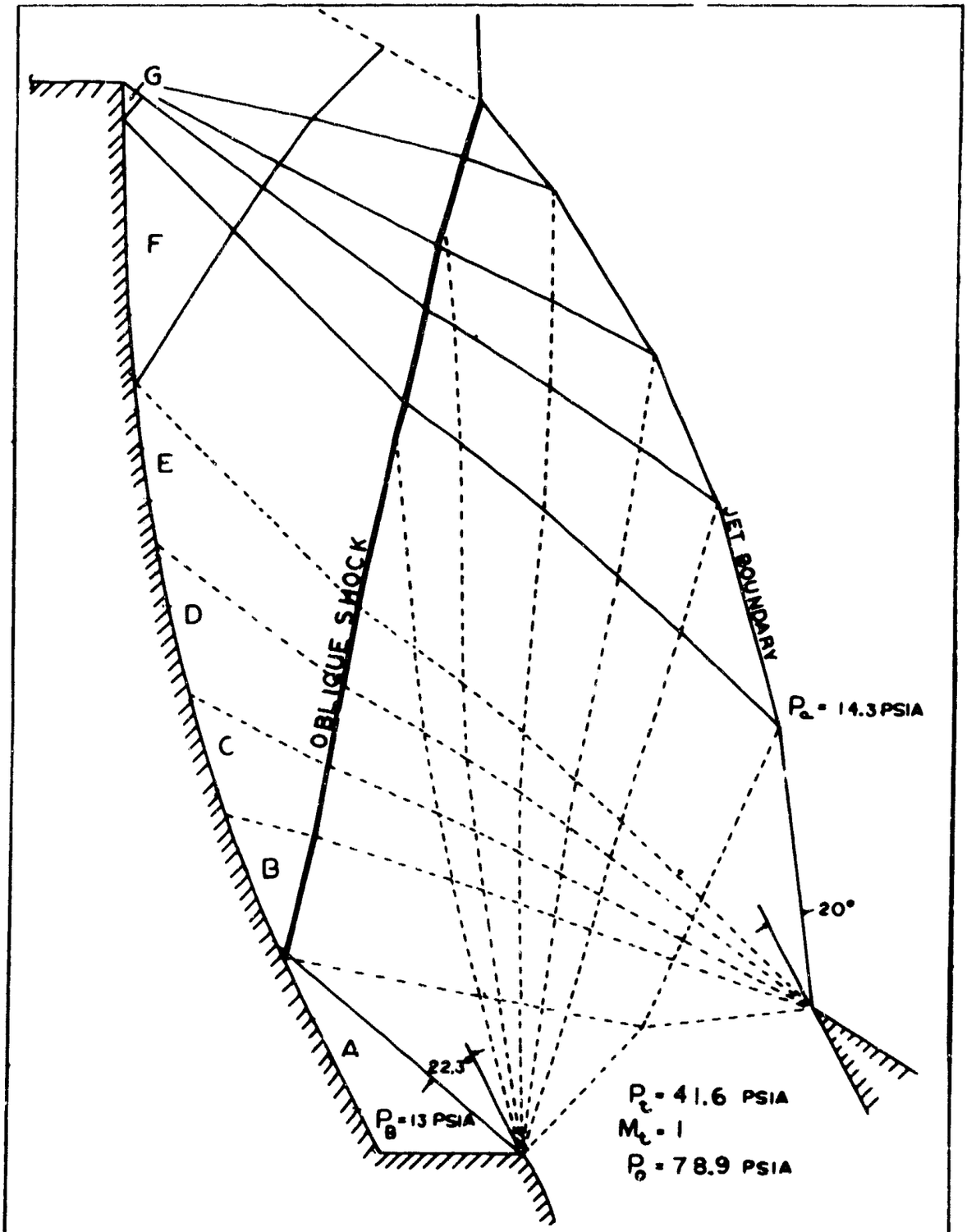

Fig. 4

Method of Characteristics Solution No. 2, P_0/P_a = 5.53

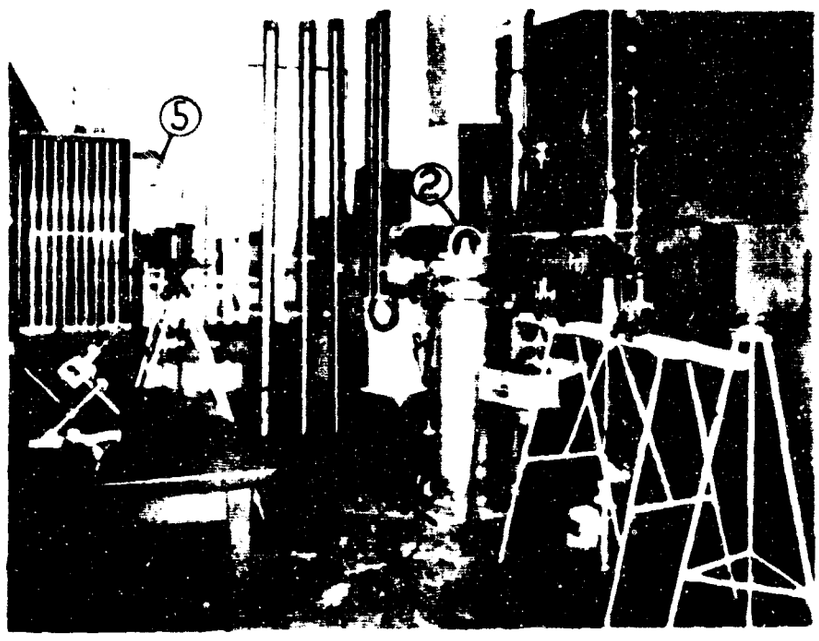

Fig. 5

General Laboratory Arrangement of Apparatus

(1) Settling Chamber

(2) Test Section

(3) Flow-Meter

(4) Schlieren Apparatus

(5) Manometer Banks

a. Location of Test Section on Vertical Settling Chamber

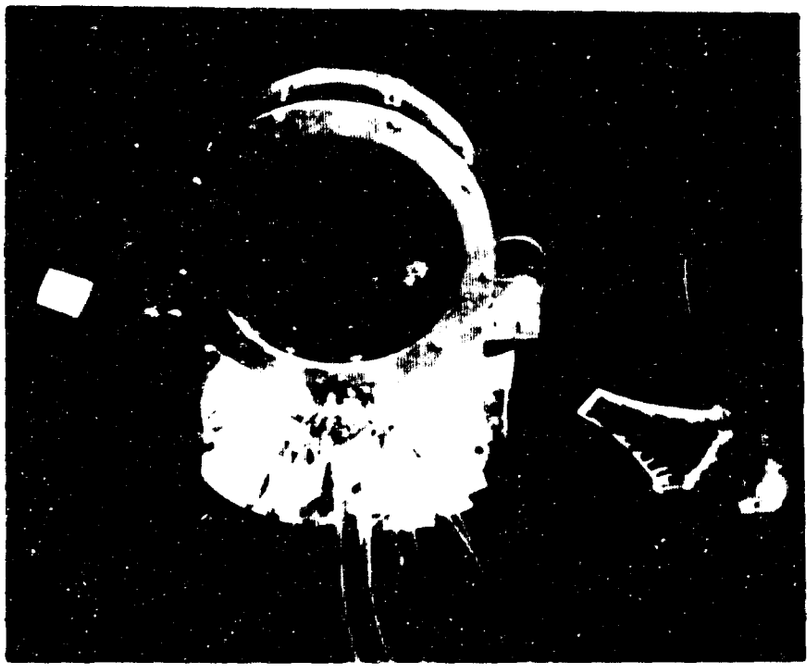

b. Test Section and Plug Assemblies

Fig. 6

Test Section Apparatus

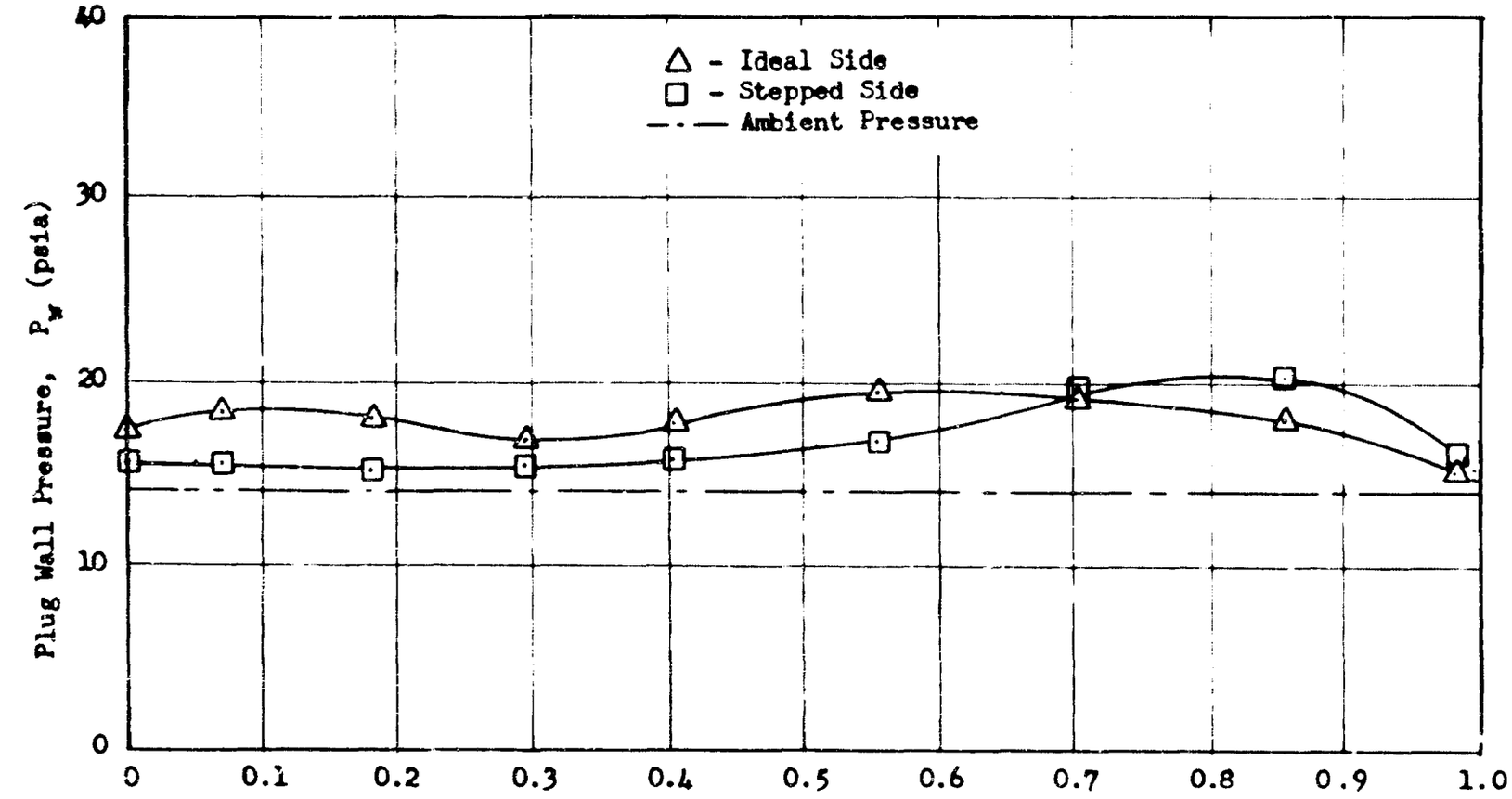

Fig. 7

Experimental Plug Wall Pressure Distribution for Translated Plug, $P_o/P_a = 2.72$

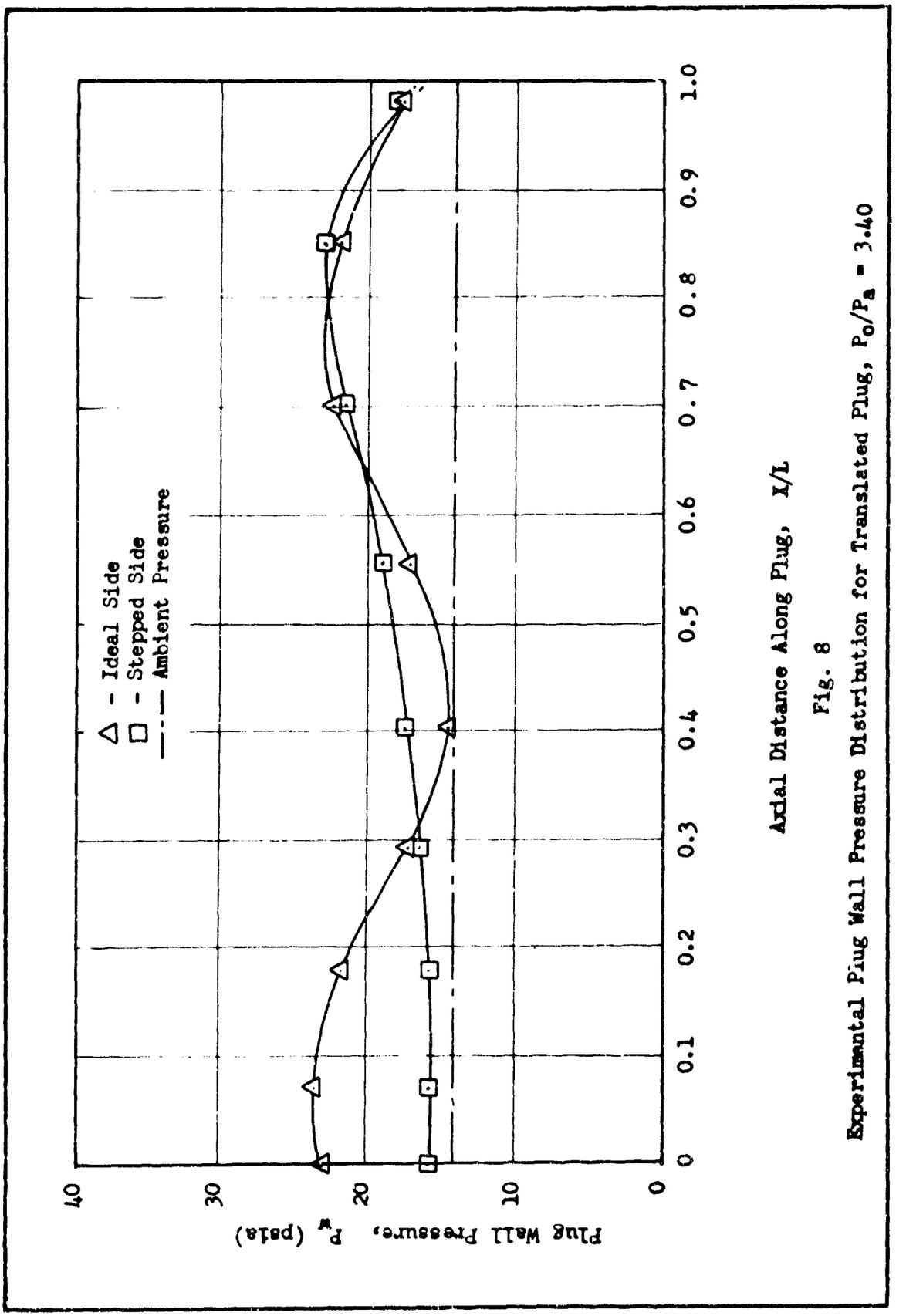

Fig. 8

Experimental Plug Wall Pressure Distribution for Translated Plug, $P_o/P_a = 3.40$

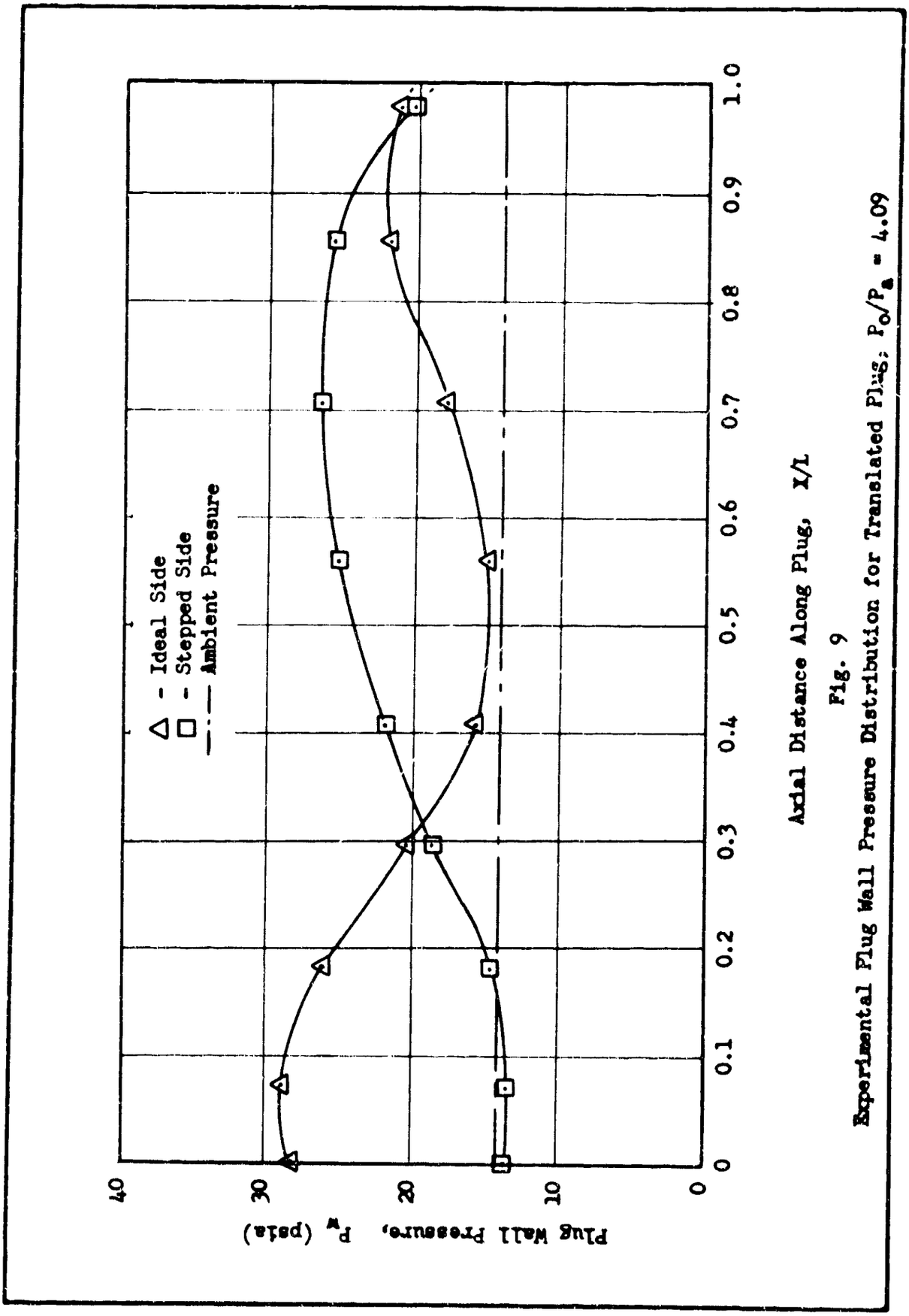

Fig. 9
Experimental Plug Wall Pressure Distribution for Translated Plug; $P_o/P_a = 4.09$

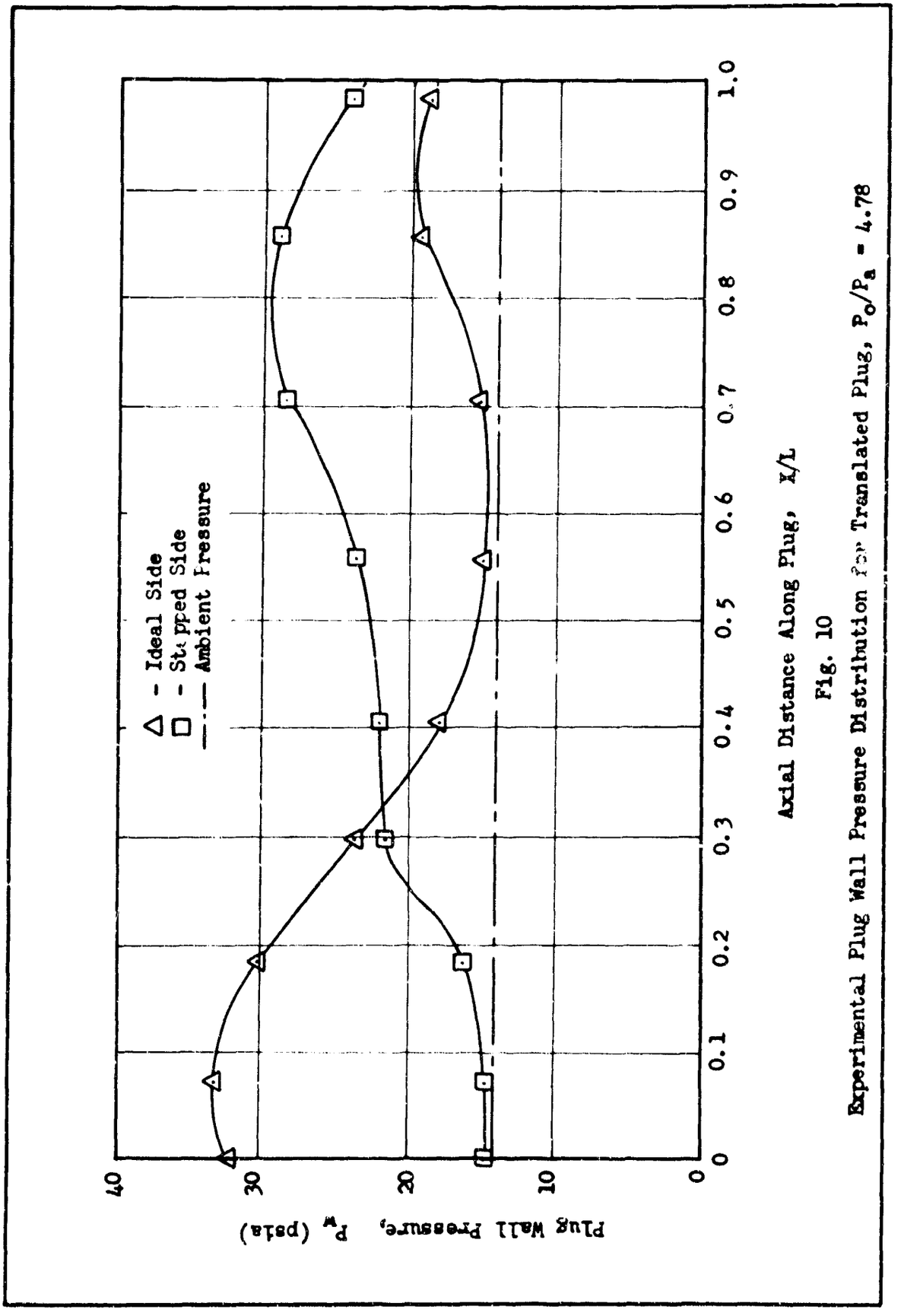

Fig. 10

Experimental Plug Wall Pressure Distribution For Translated Plug, $P_o/P_a = 4.78$

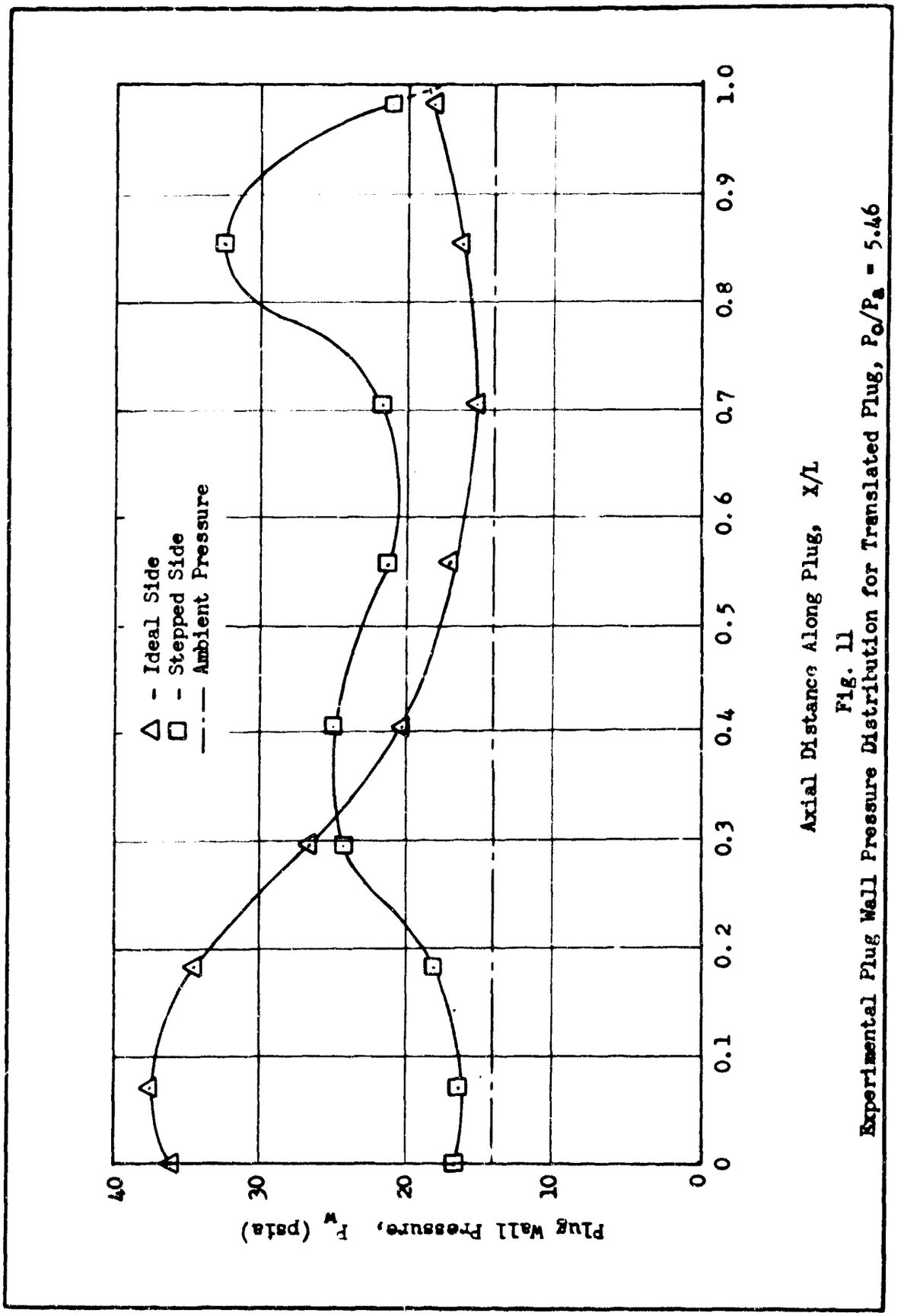

Fig. 11
Experimental Plug Wall Pressure Distribution for Translated Plug, $P_o/P_a = 5.46$

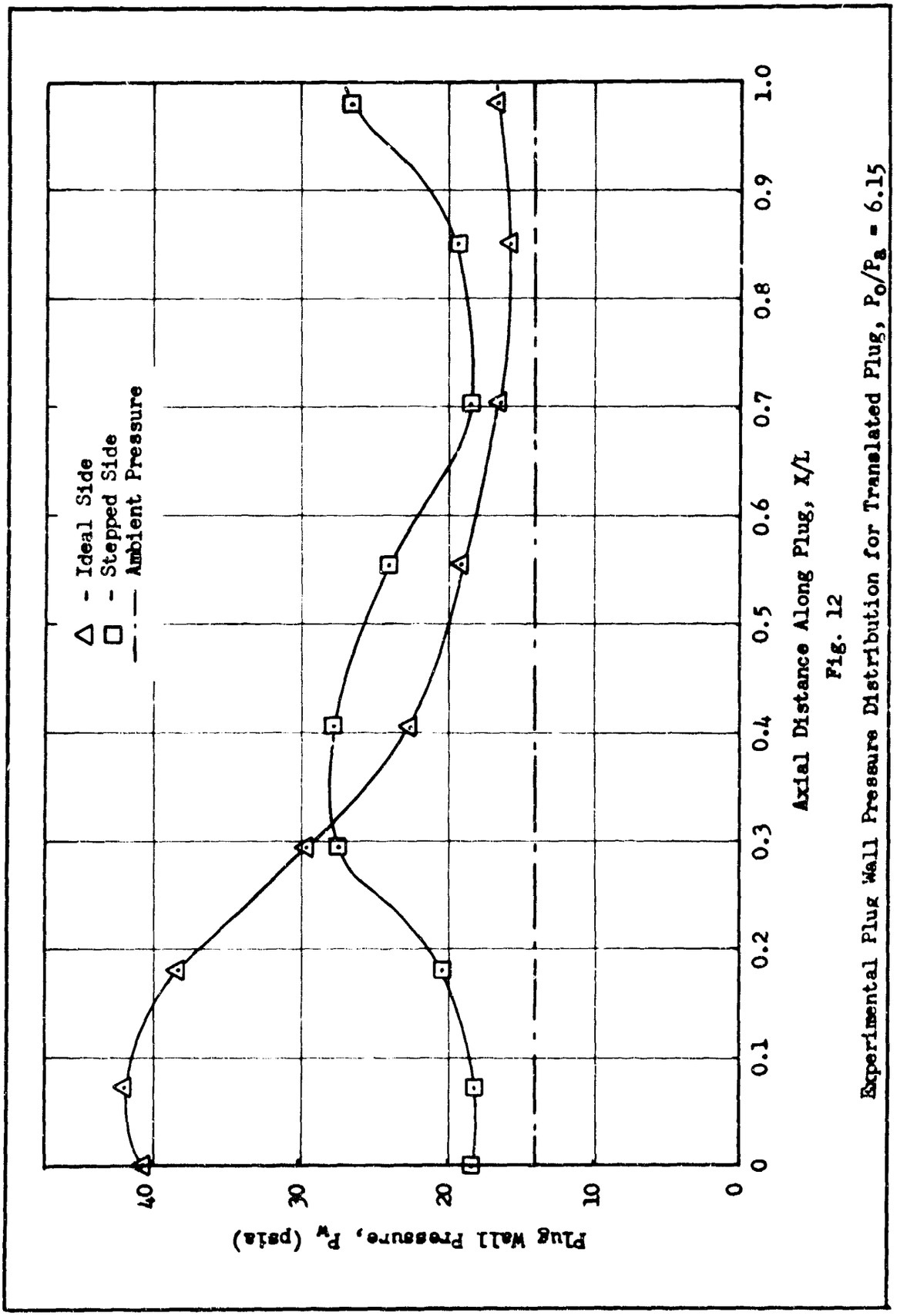

Fig. 12

Experimental Plug Wall Pressure Distribution for Translated Plug, $P_o/P_a = 6.15$

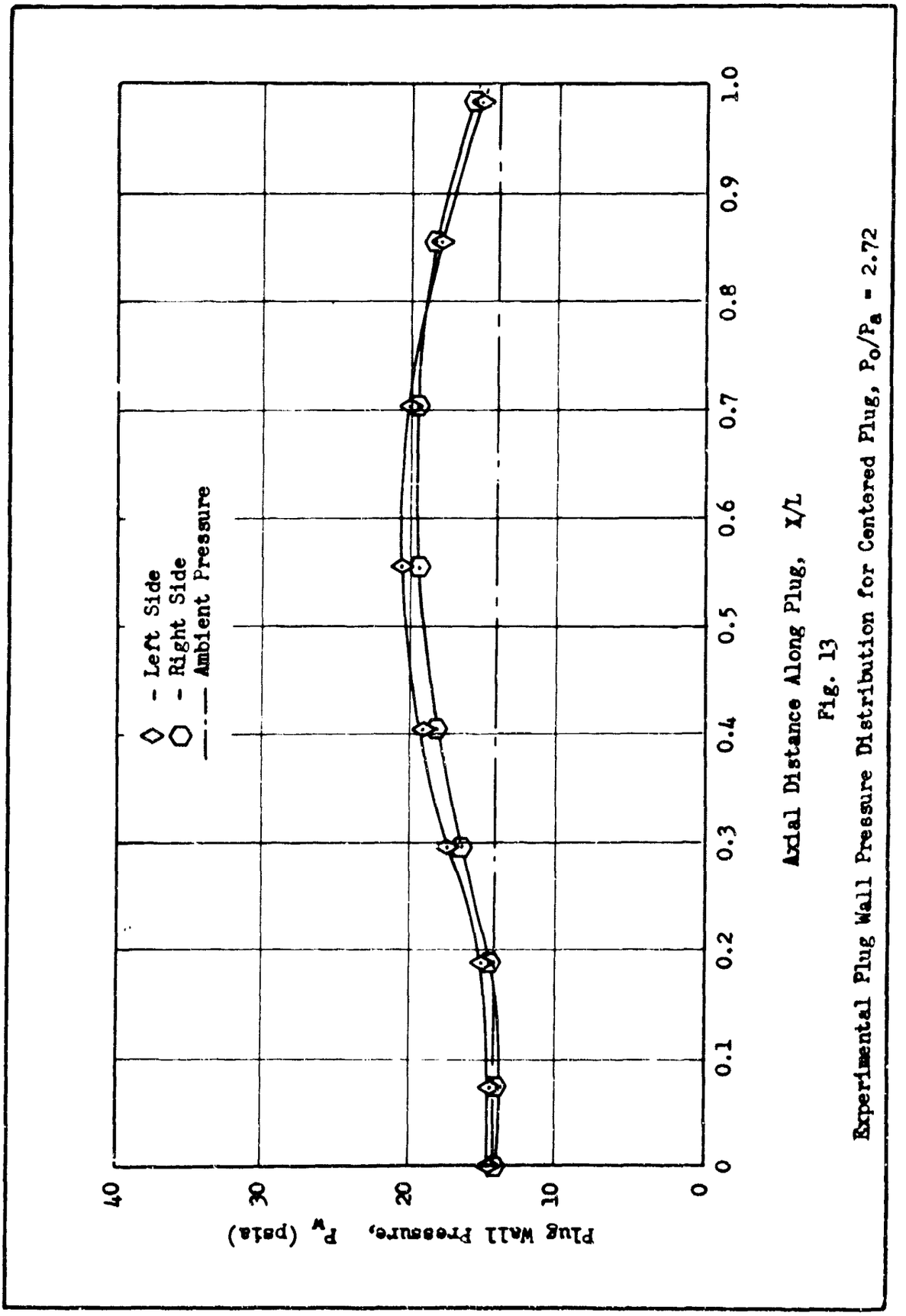

Fig. 13

Experimental Plug Wall Pressure Distribution for Centered Plug, $P_o/P_a = 2.72$

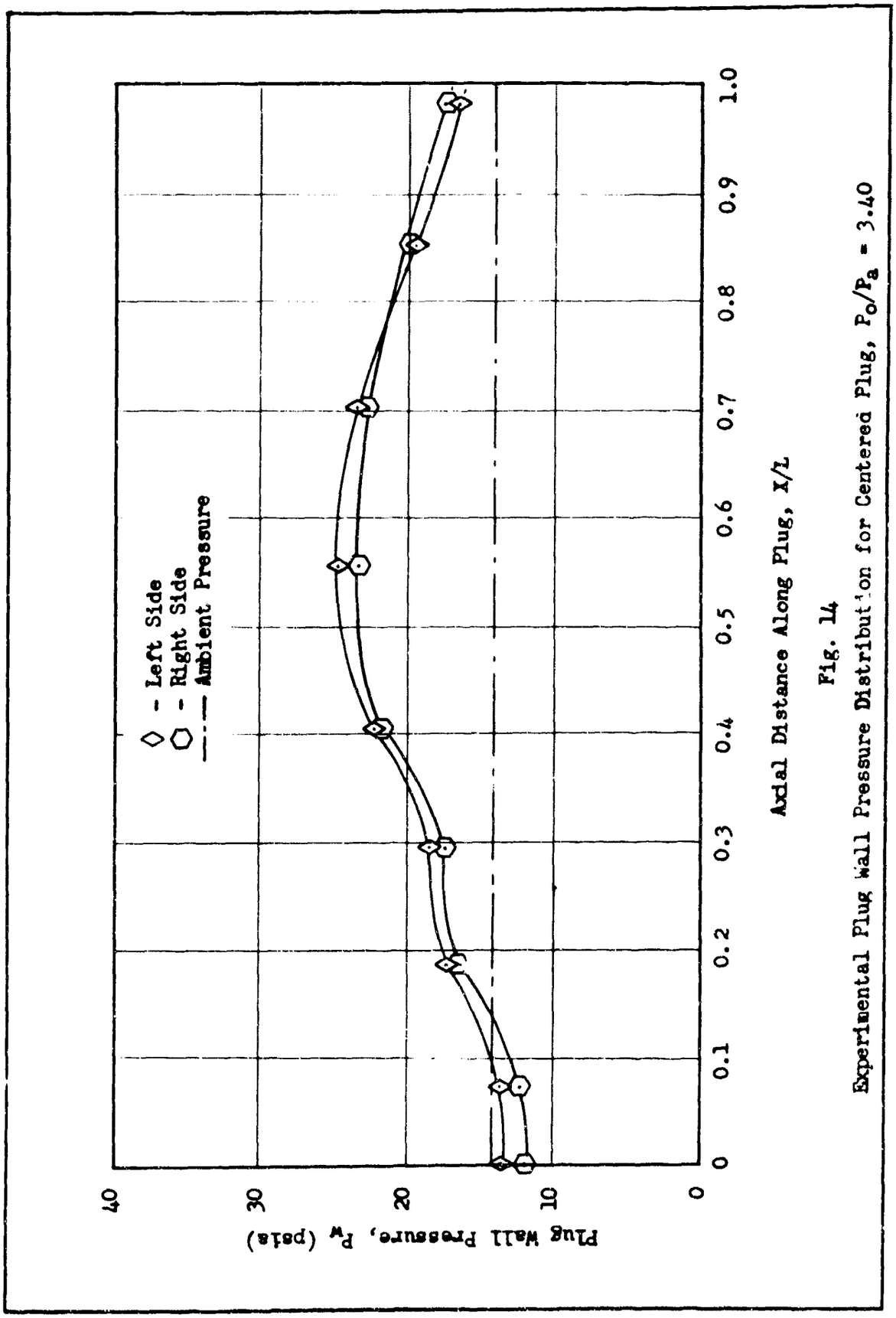

Fig. 14

Experimental Plug Wall Pressure Distribution for Centered Plug, $P_o/P_a = 3.40$

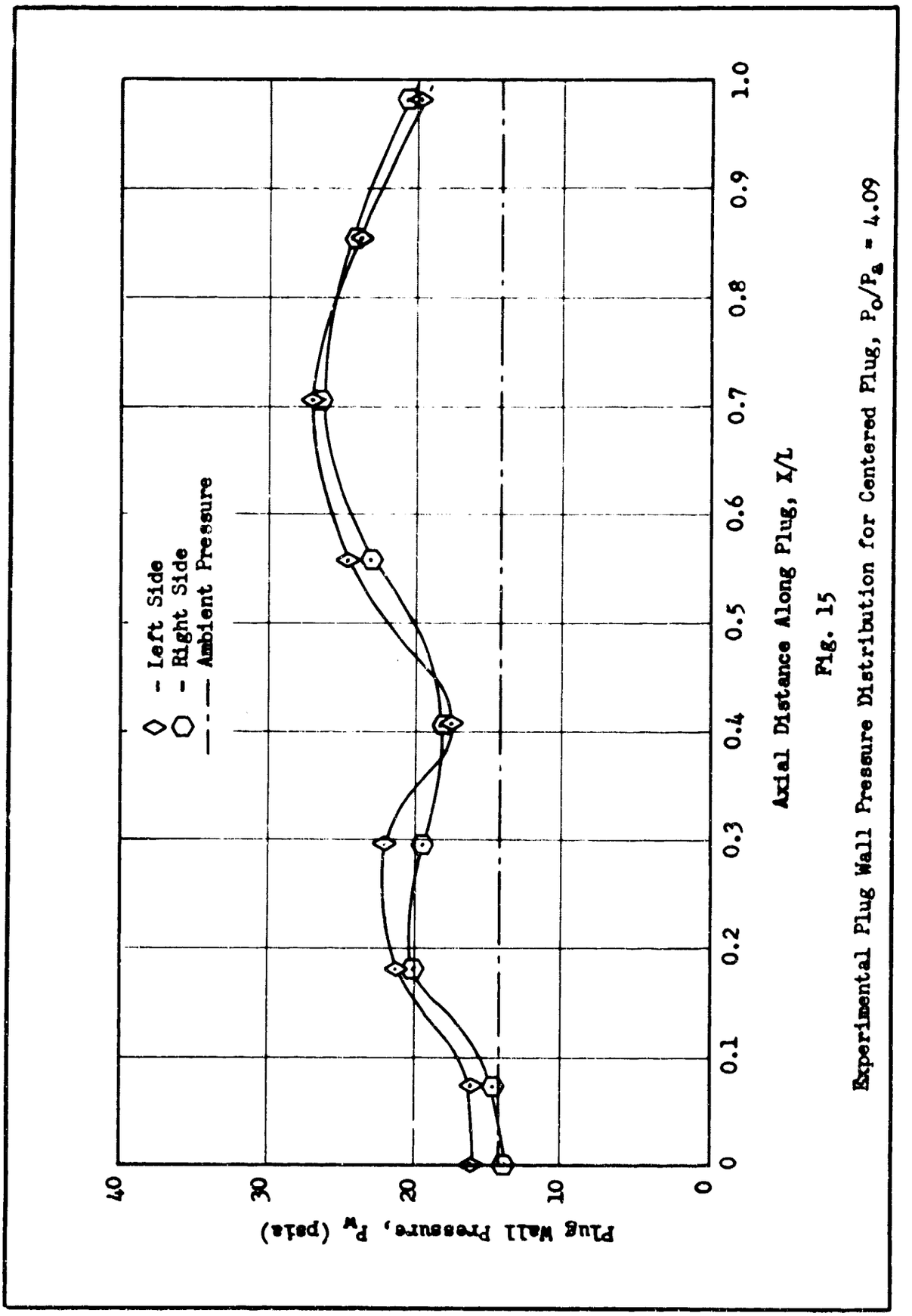

Fig. 15

Experimental Plug Wall Pressure Distribution for Centered Plug, $P_o/P_a = 4.09$

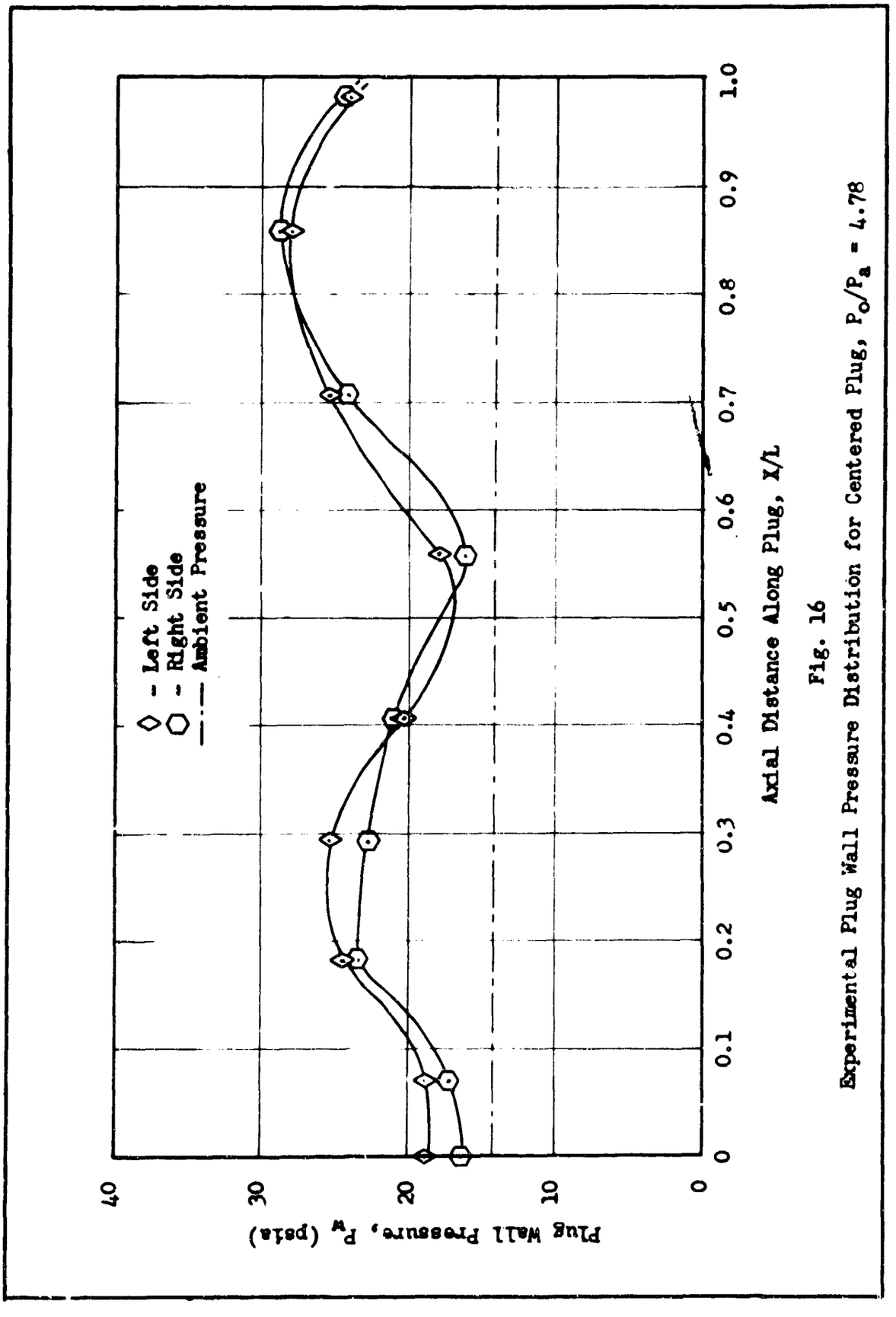

Fig. 16

Experimental Plug Wall Pressure Distribution for Centered Plug, $P_o/P_a = 4.78$

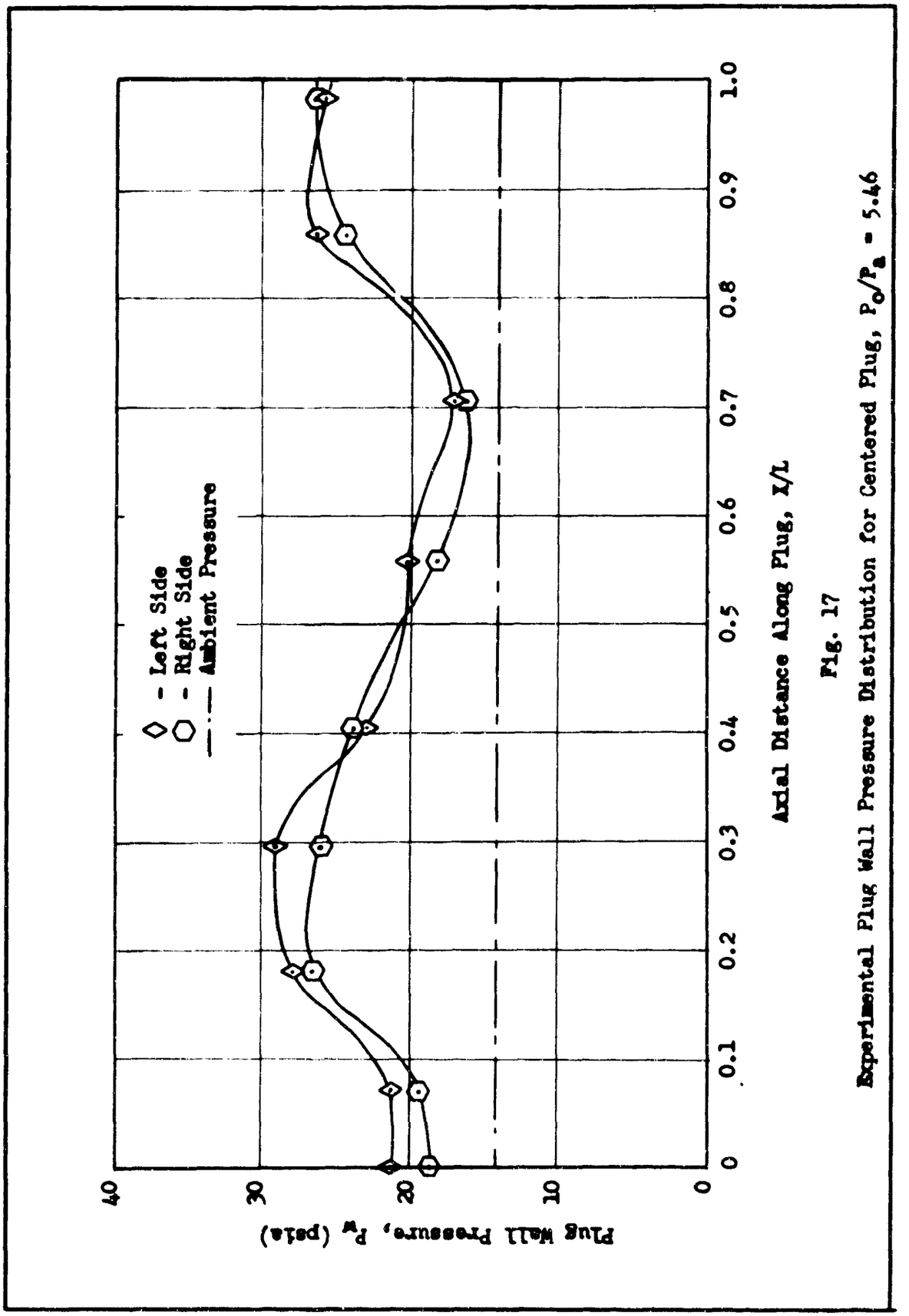

Fig. 17

Experimental Plug Wall Pressure Distribution for Centered Plug, P_o/P_a = 5.46

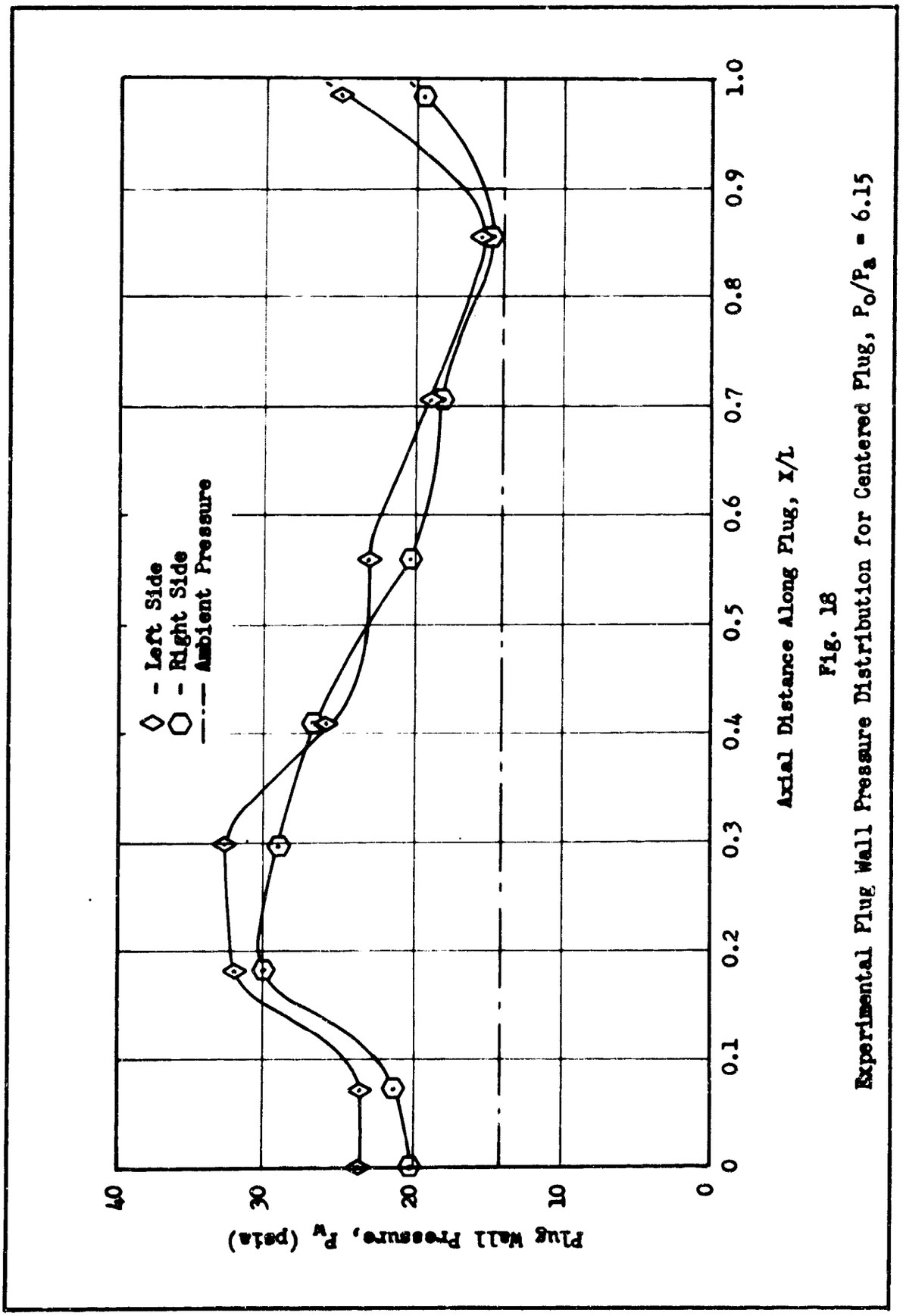

Fig. 18

Experimental Plug Wall Pressure Distribution for Centered Plug, $P_o/P_a = 6.15$

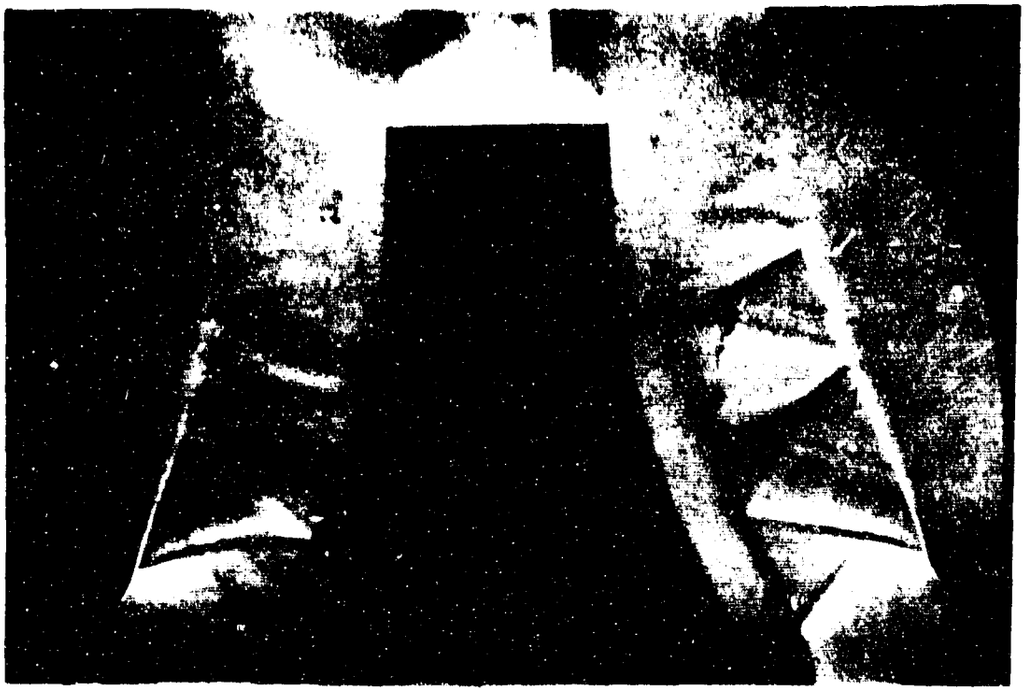

a. Translated Plug: $P_o/P_a = 2.72$

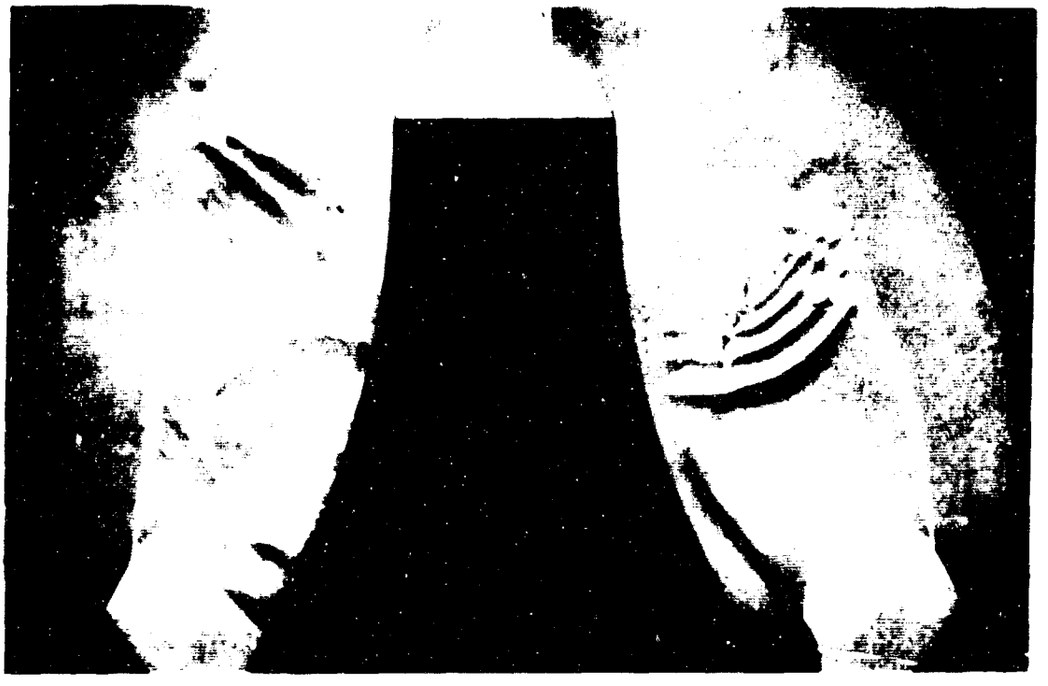

b. Translated Plug: $P_o/P_a = 4.09$

Fig. 19

Schlieren Photographs of Translated Plug

a. Translated Plug: $P_o/P_a = 4.78$

b. Translated Plug: $P_o/P_a = 5.46$

Fig. 20
Schlieren Photographs of Translated Plug

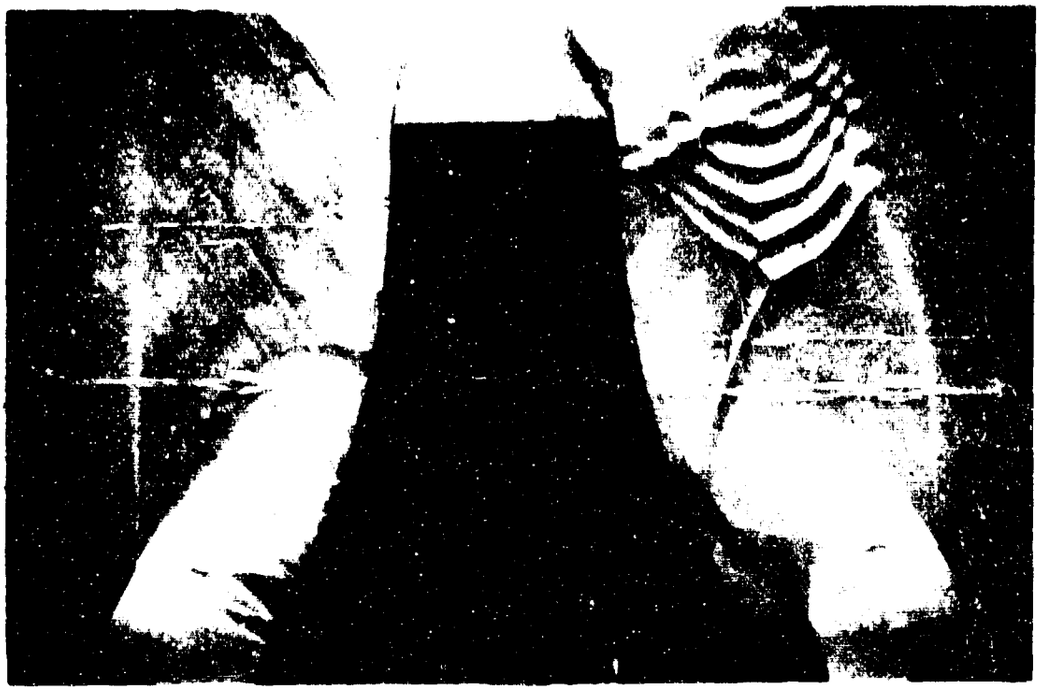

a. Translated Plug: $P_o/P_a = 6.15$

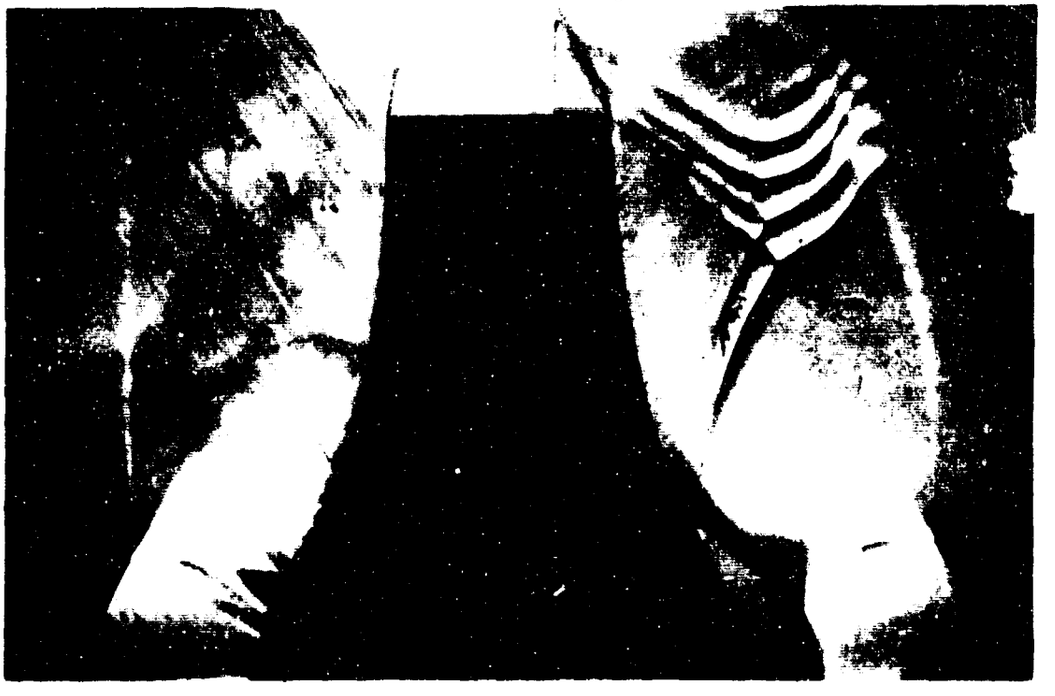

b. Translated Plug: $P_o/P_a = 6.50$

Fig. 21
Schlieren Photographs of Translated Plug

a. Centered Plug: $P_o/P_a = 2.72$

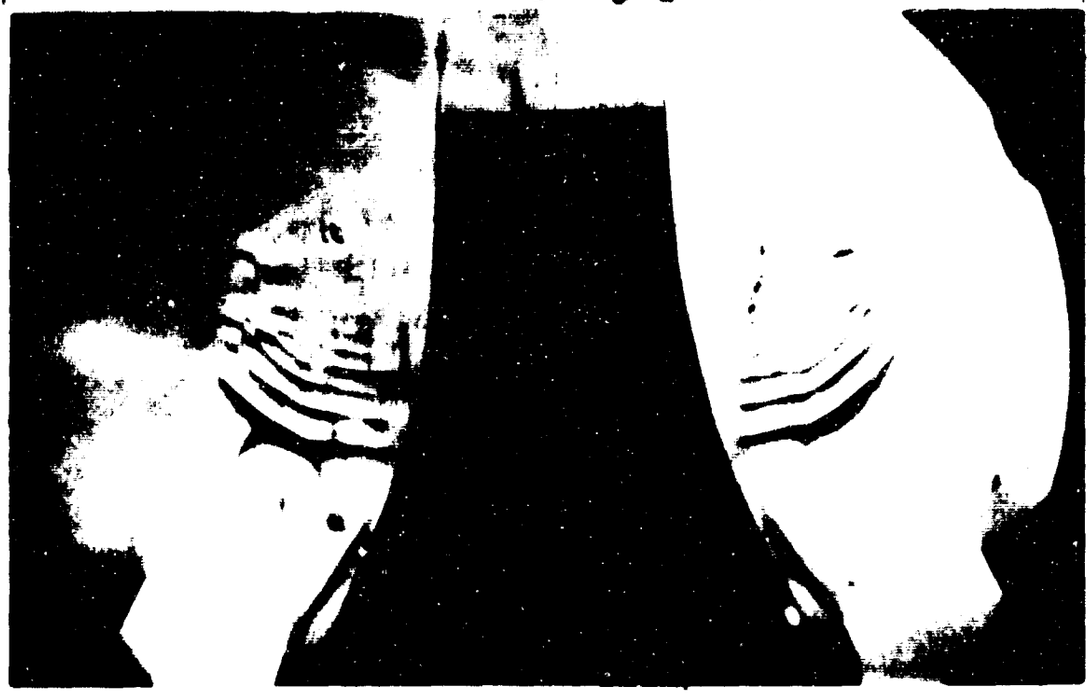

b. Centered Plug: $P_o/P_a = 3.40$

Fig. 22
Schlieren Photographs of Centered Plug

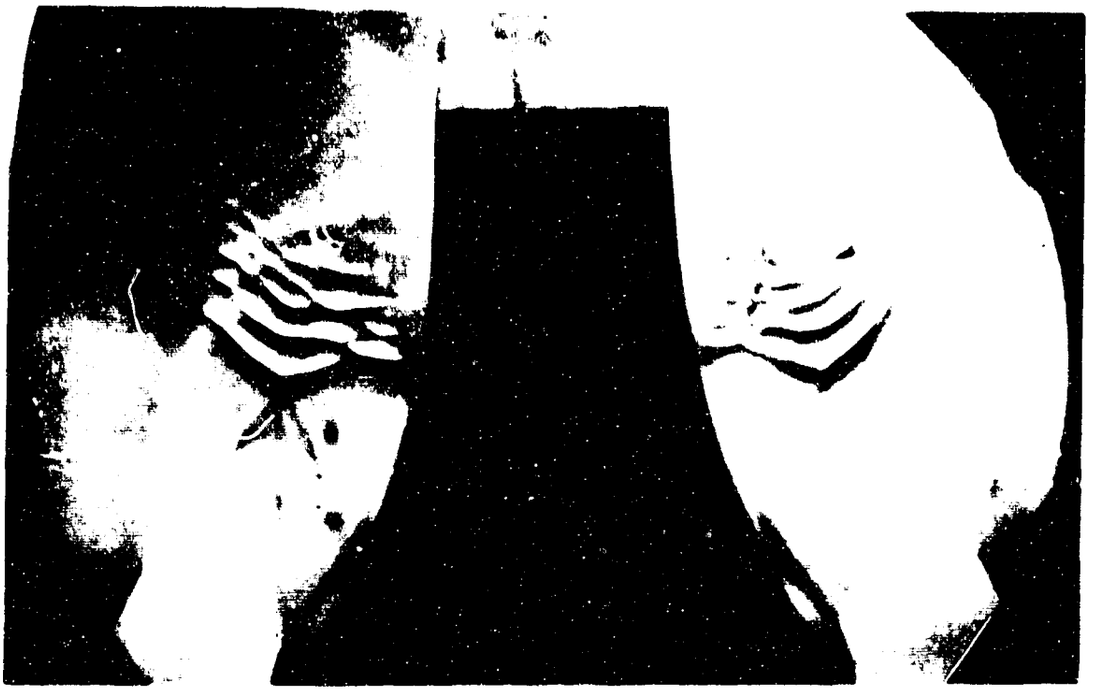

a. Centered Plug: $P_o/P_a = 4.09$

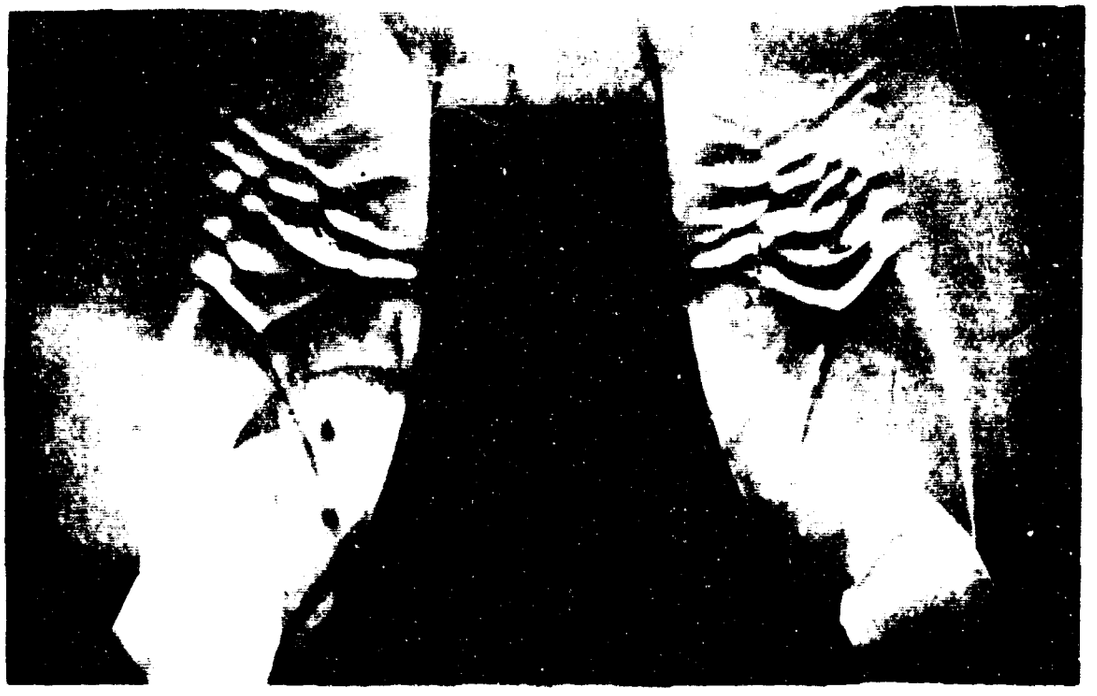

b. Centered Plug: $P_o/P_a = 4.78$

Fig. 23
Schlieren Photographs of Centered Plug

a. Centered Plug: $P_o/P_a = 5.46$

b. Centered Plug: $P_o/P_a = 6.60$

Fig. 24
Schlieren Photographs of Centered Plug

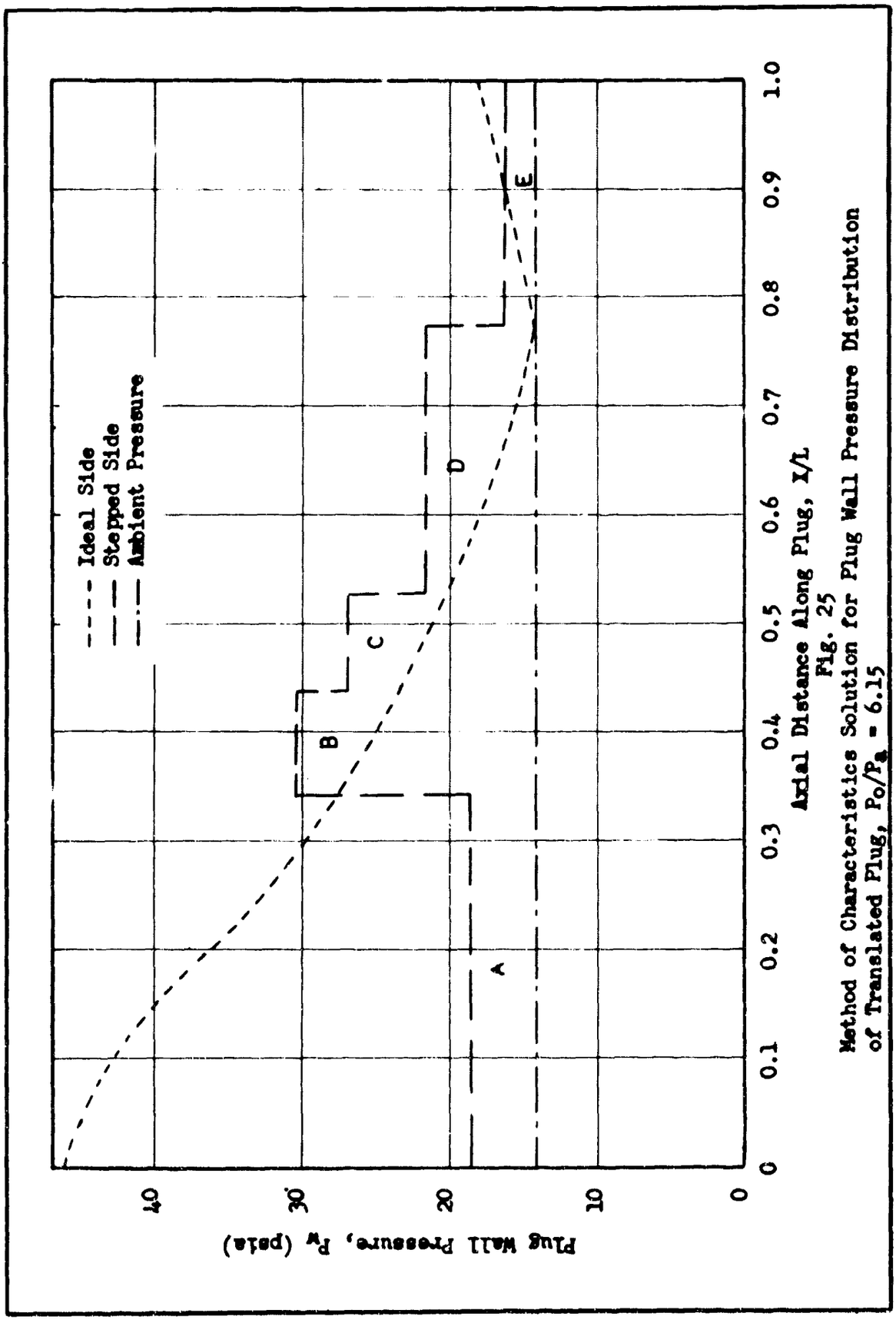

Fig. 25
Method of Characteristics Solution for Plug Wall Pressure Distribution of Translated Plug, $P_o/P_a = 6.15$

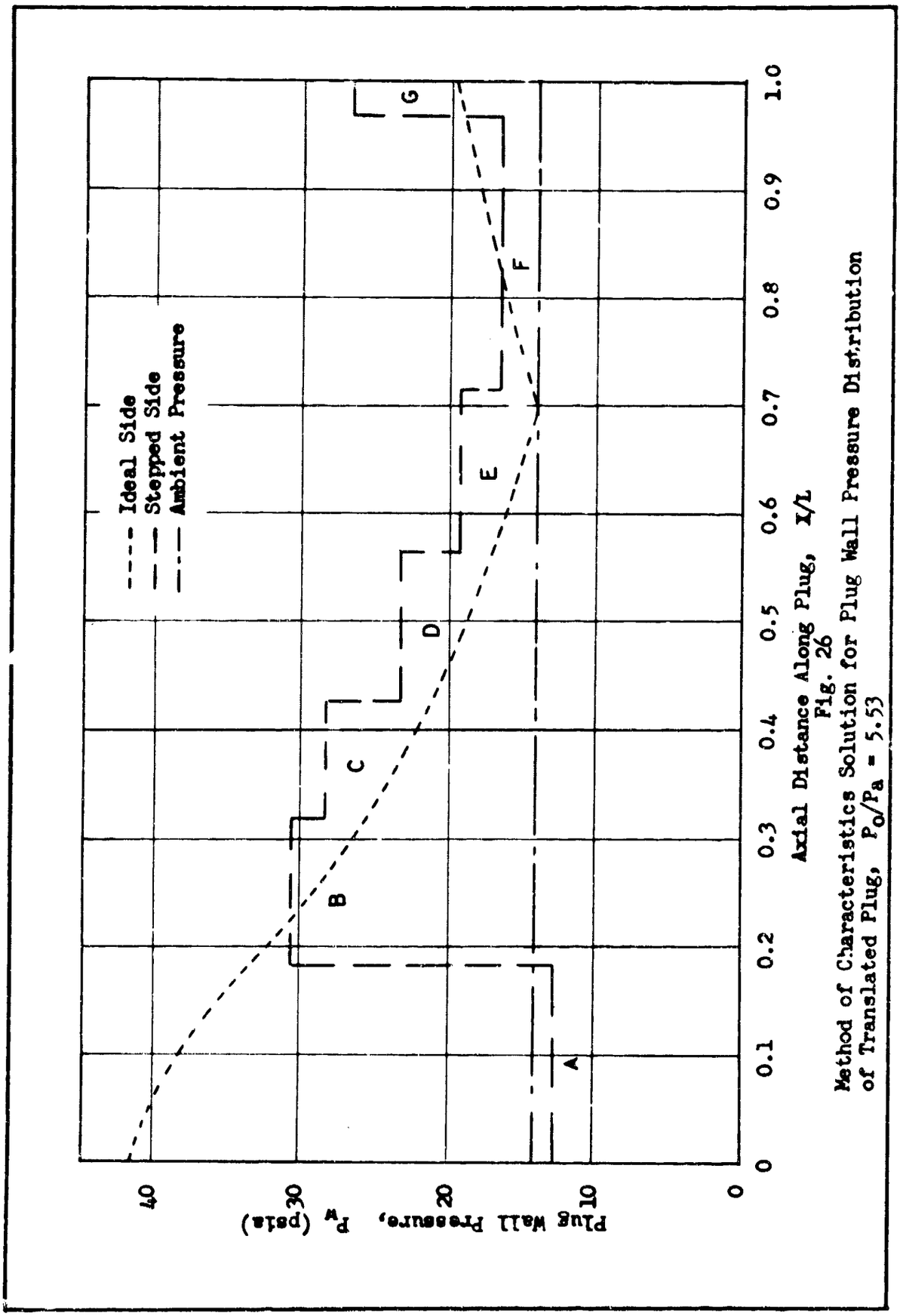

Method of Characteristics Solution for Plug Wall Pressure Distribution of Translated Plug, $P_o/P_a = 5.53$

Fig. 26

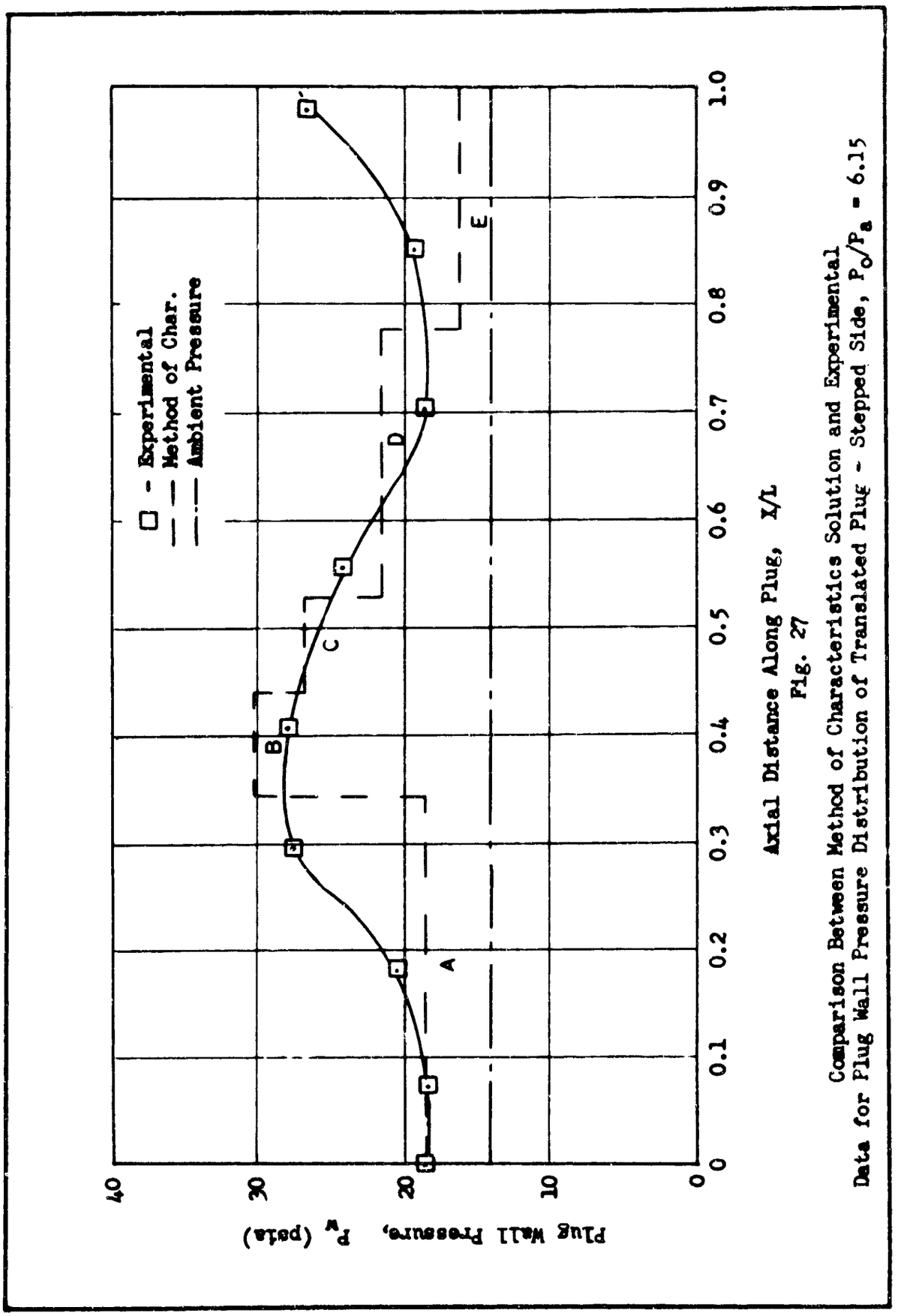

Fig. 27

Comparison Between Method of Characteristics Solution and Experimental Data for Plug Wall Pressure Distribution of Translated Plug - Stepped Side, P_o/P_a = 6.15

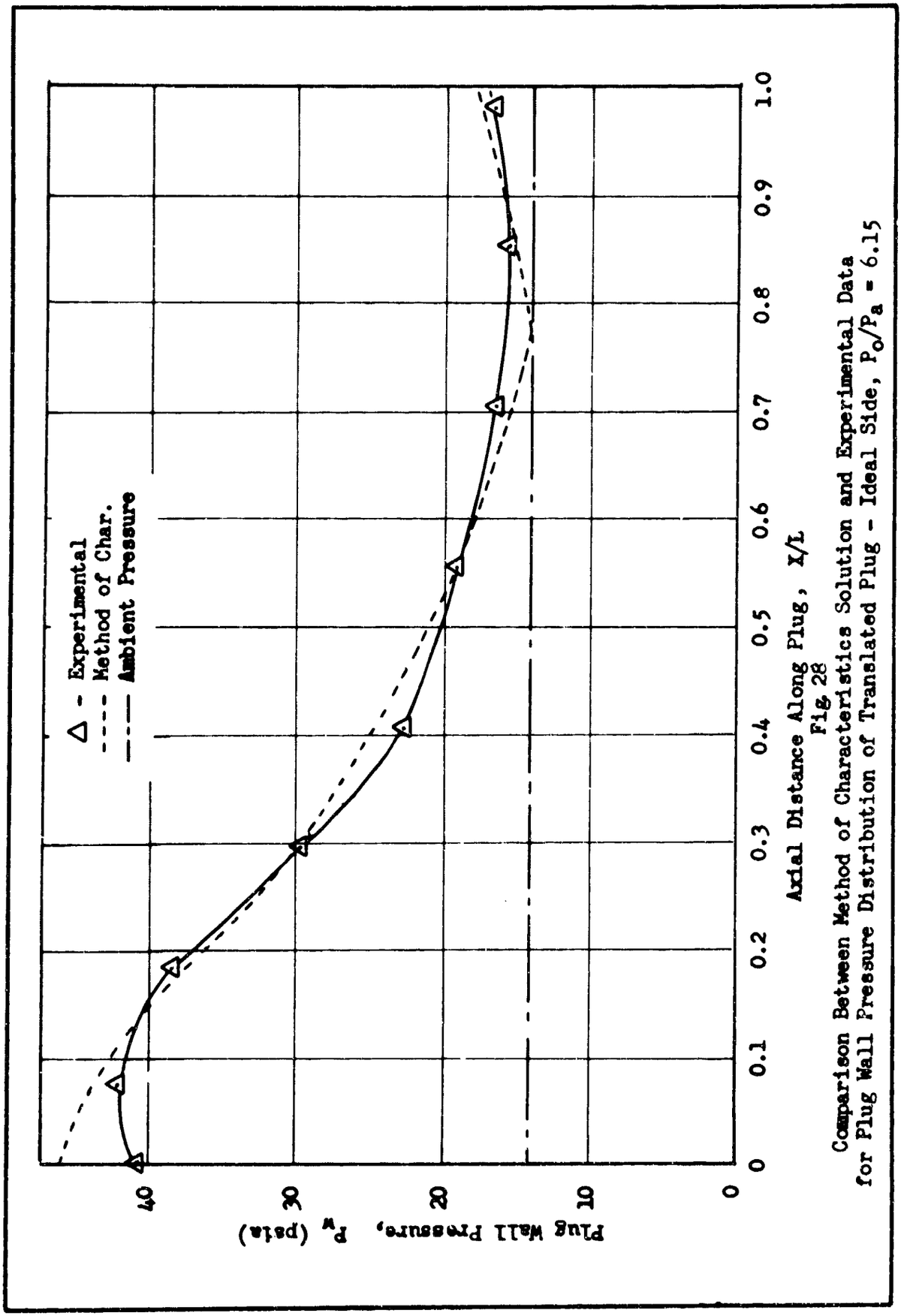

Fig 28

Comparison Between Method of Characteristics Solution and Experimental Data for Plug Wall Pressure Distribution of Translated Plug - Ideal Side, $P_o/P_a = 6.15$

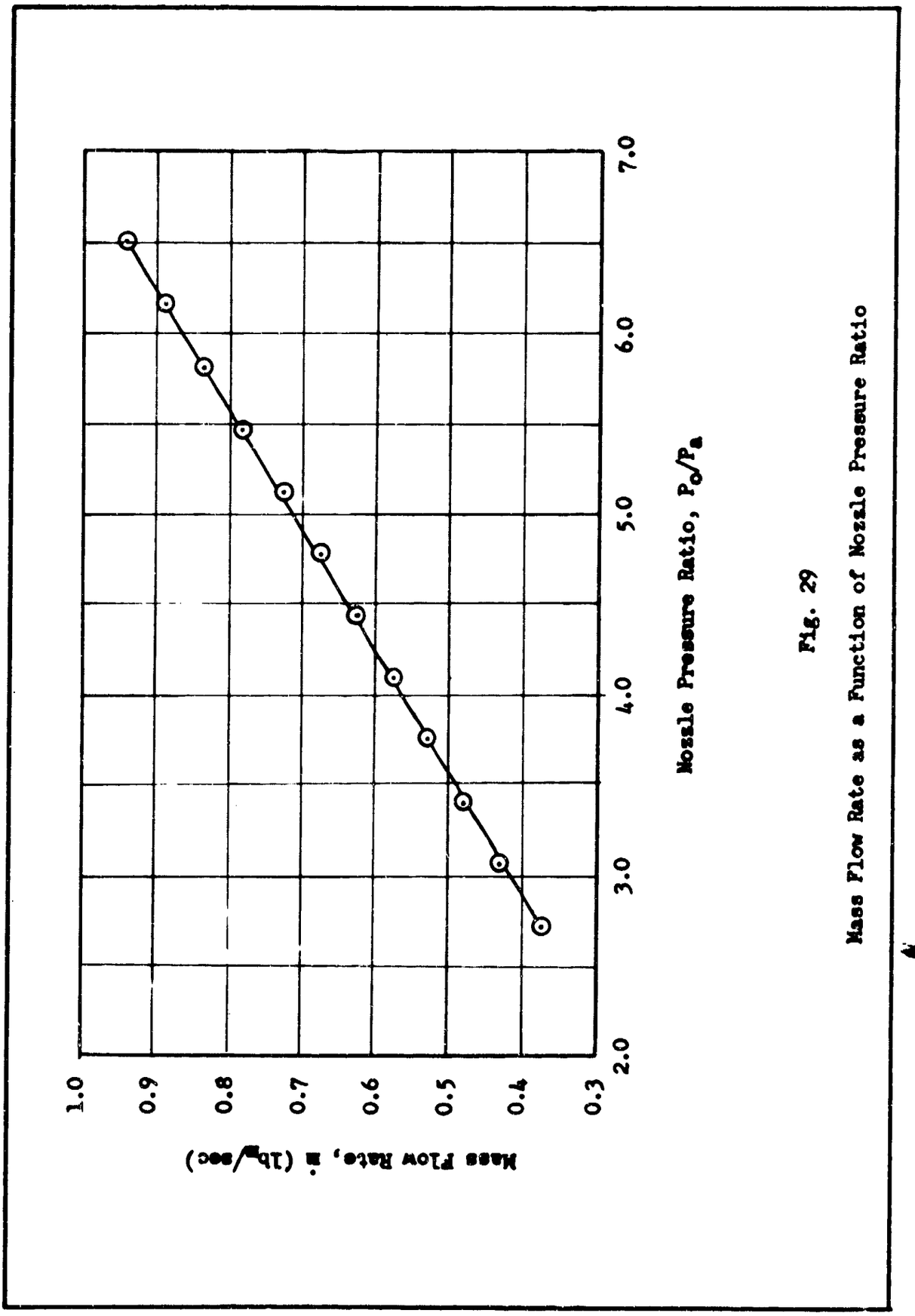

Fig. 29

Mass Flow Rate as a Function of Nozzle Pressure Ratio

Fig. 30

Variation of Thrust Vectoring With Pressure Ratio

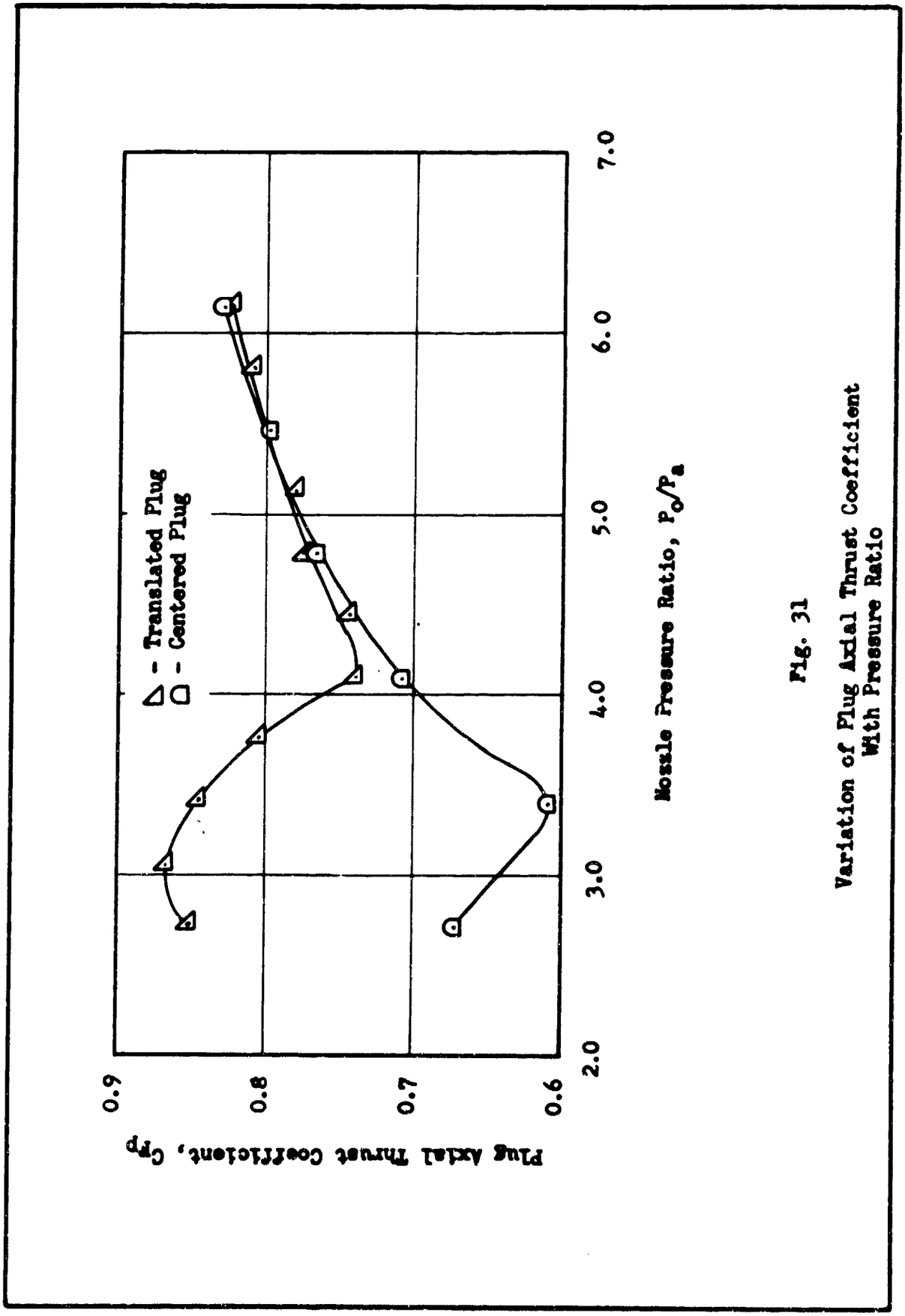

Fig. 31

Variation of Plug Axial Thrust Coefficient With Pressure Ratio

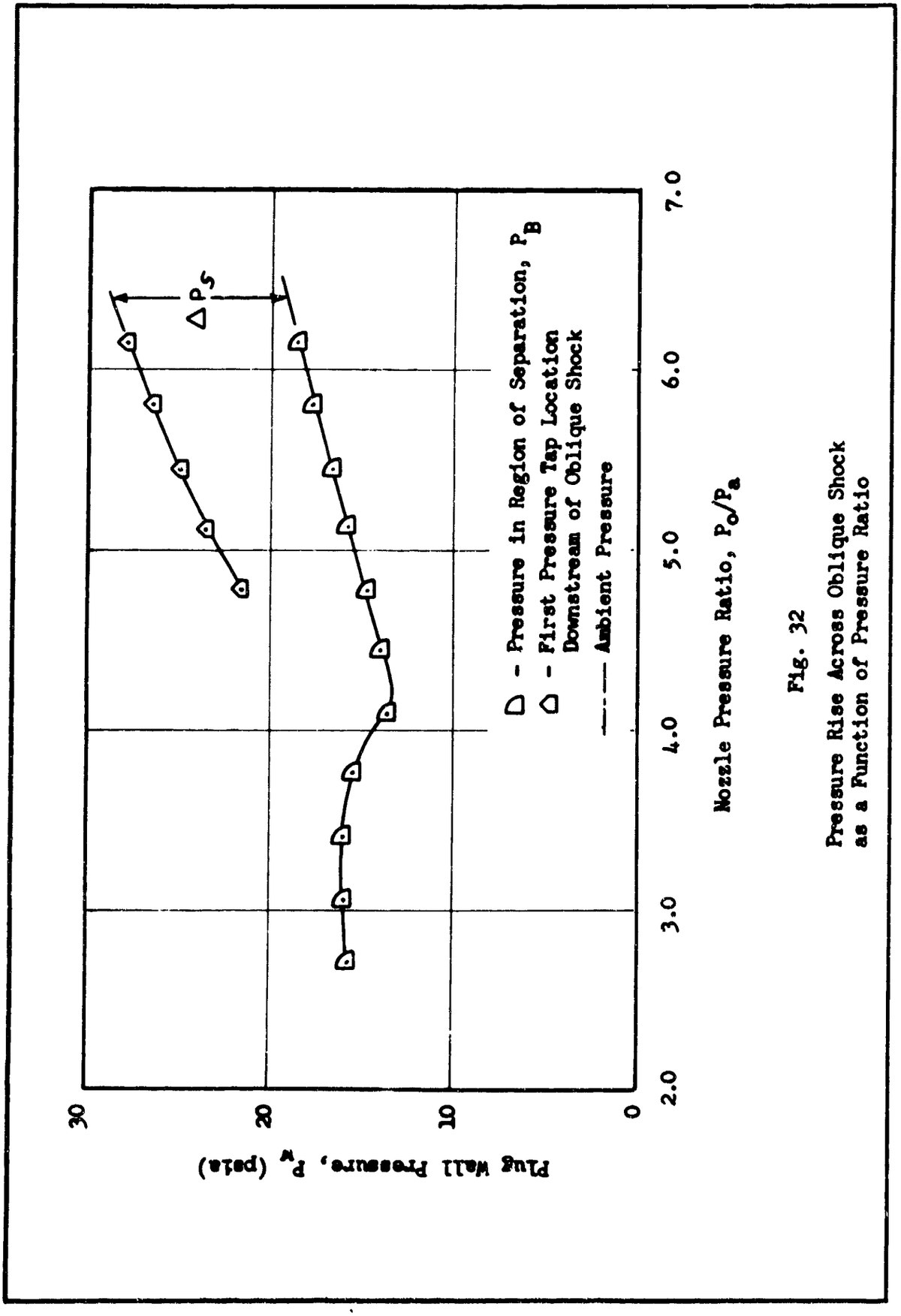

Fig. 32

Pressure Rise Across Oblique Shock as a Function of Pressure Ratio

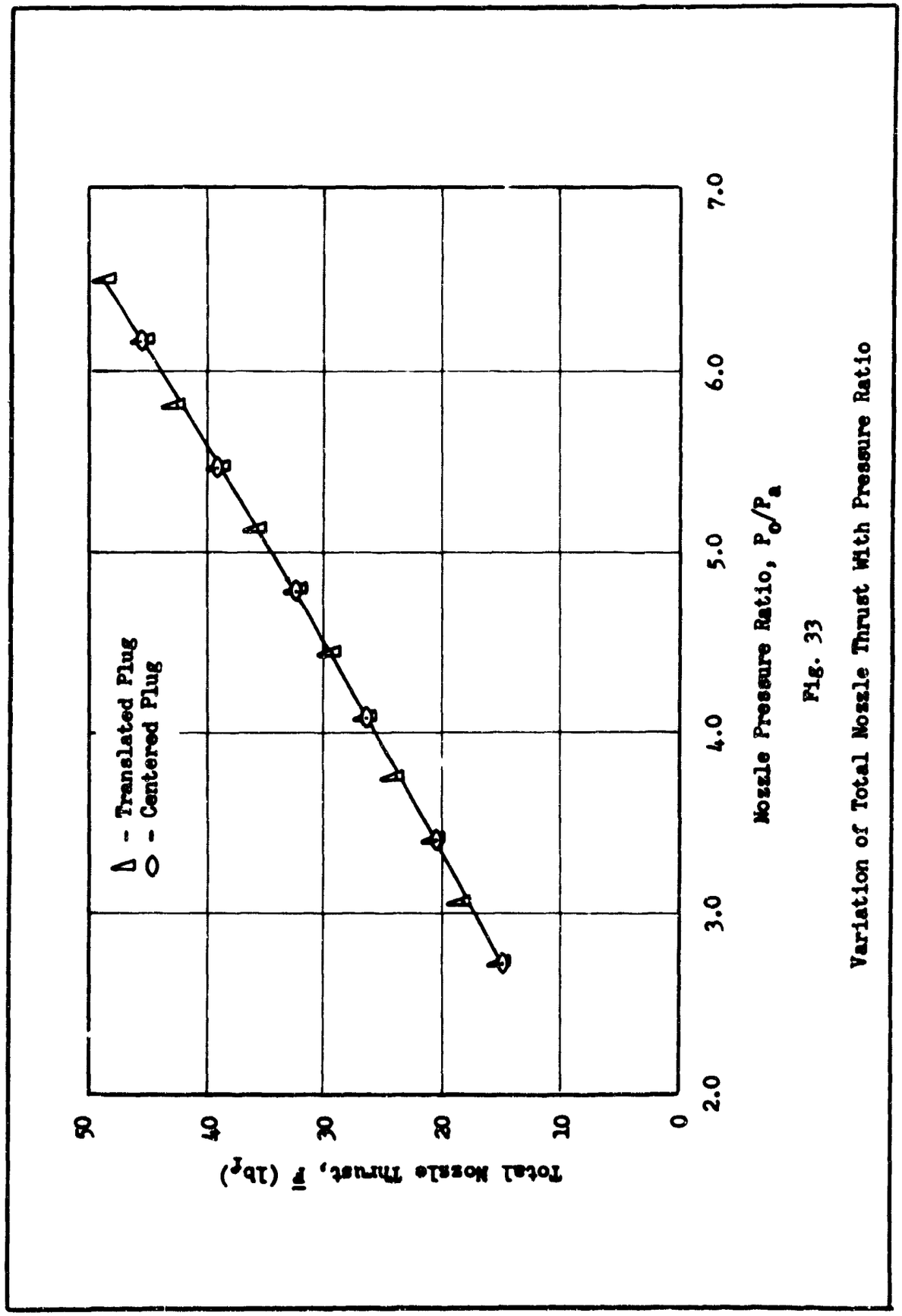

Fig. 33

Variation of Total Nozzle Thrust With Pressure Ratio

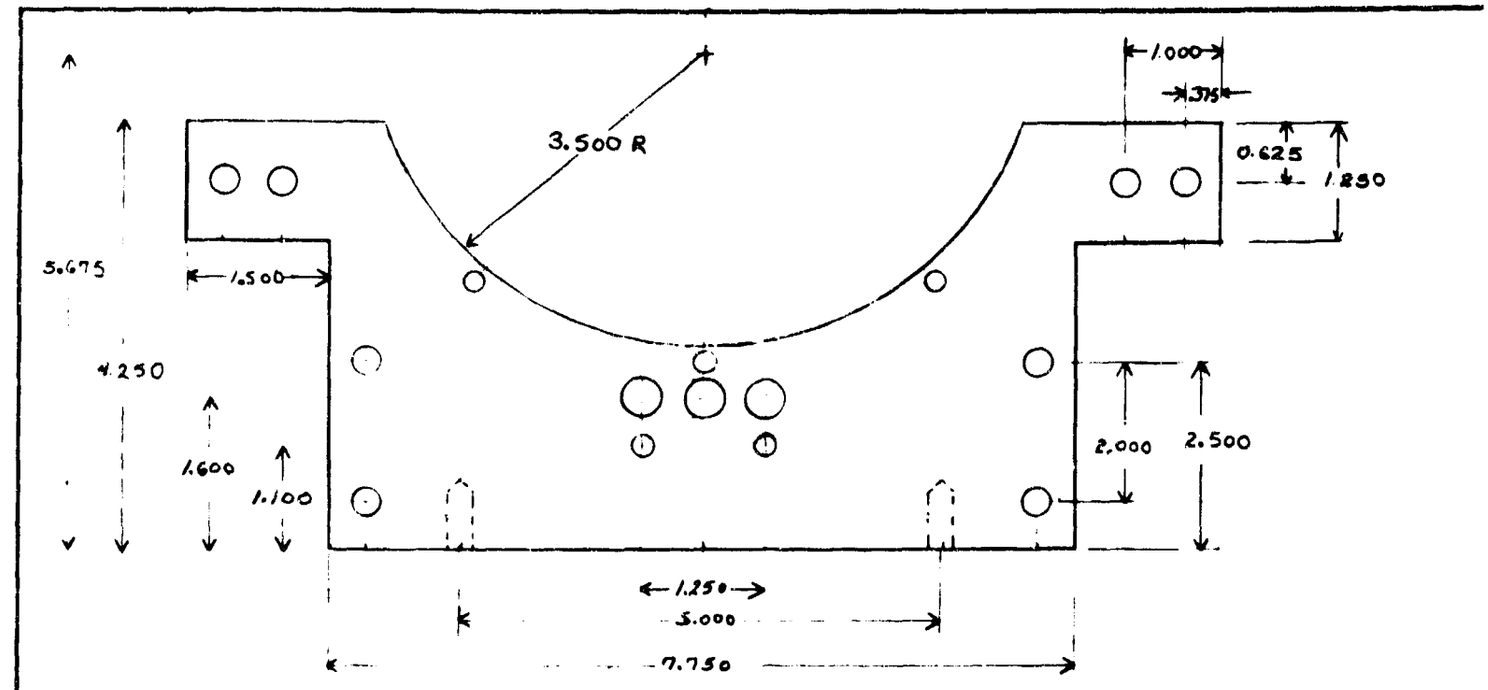

PART NO. 1 FRONT SIDE PLATE
THICKNESS = 0.850" MAT'L: ALUMINUM

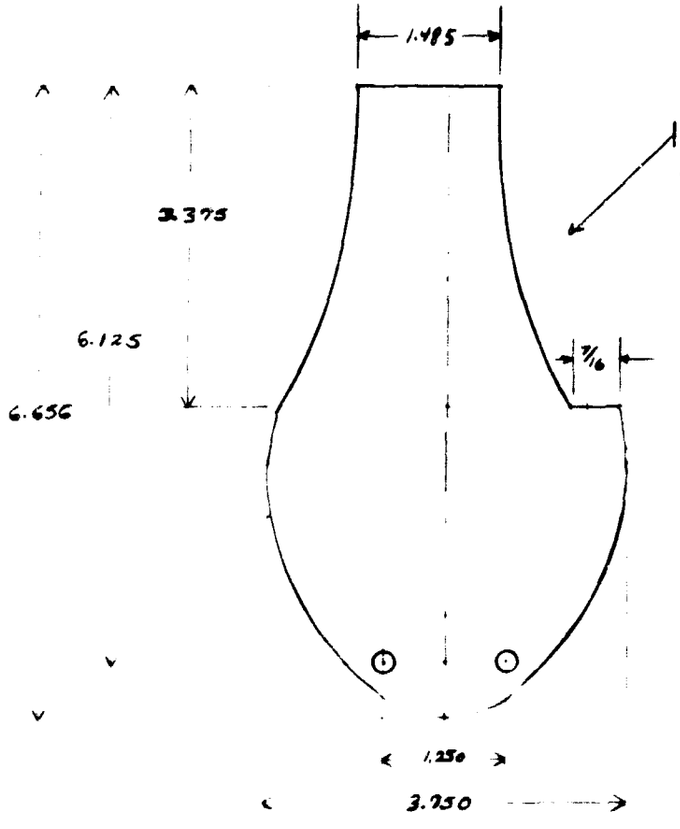

PART NO. 4 TRANSLATED PLUG. THICKNESS = 0.191"
MAT'L: BRASS

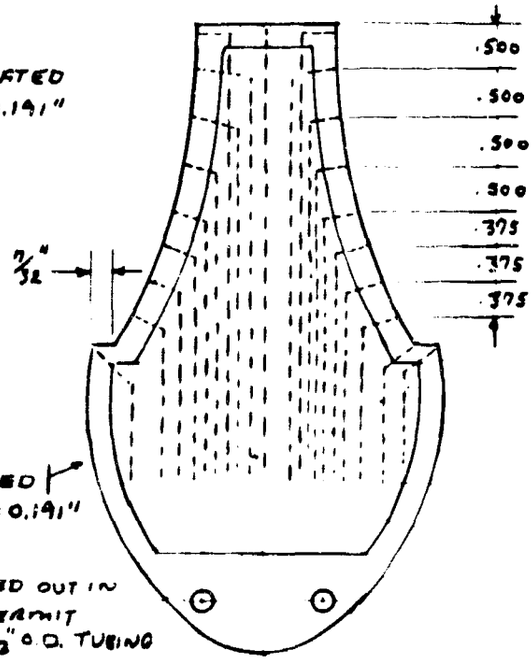

PART NO. 5 CENTERED PLUG. THICKNESS = 0.191"
MAT'L: BRASS

NOTE: CAVITY MILLED OUT IN FACE OF PLUG TO PERMIT INSTALLATION OF 1/32" O.D. TUBING

NOTE: GLASS RETAINING RINGS NOT SHOWN.

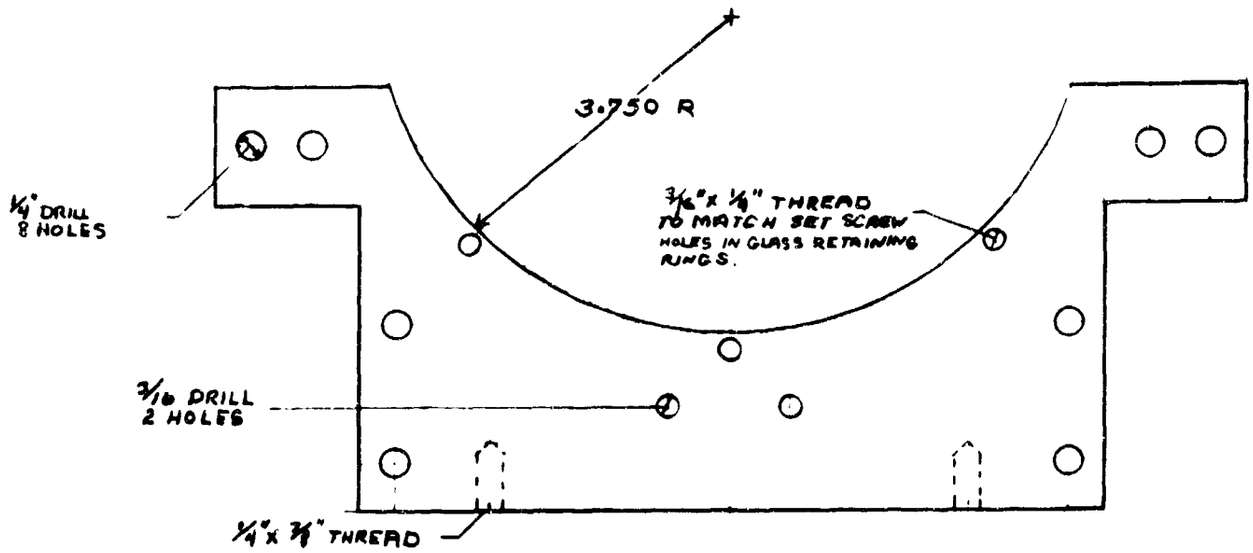

PART NO. 2 BACK SIDE PLATE
THICKNESS = 0.850" MAT'L: ALUMINUM

PART NO 3
THICKNESS = 0.

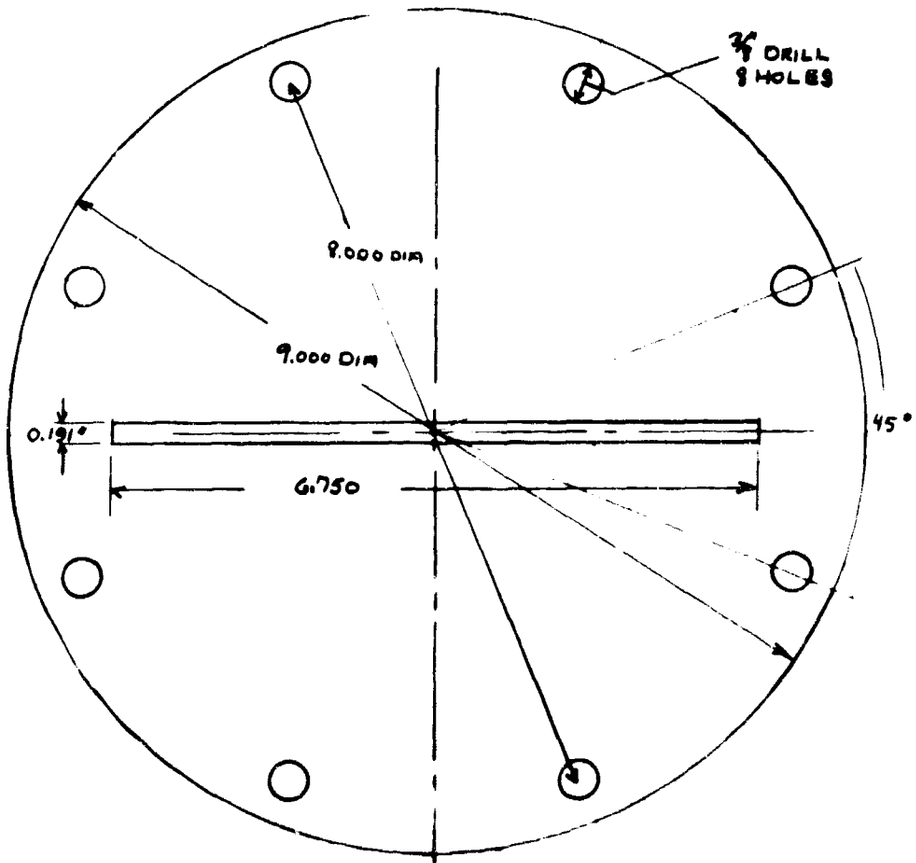

PART NO. 6 BASE PLATE
THICKNESS = 0.500" MAT'L: ALUMINUM

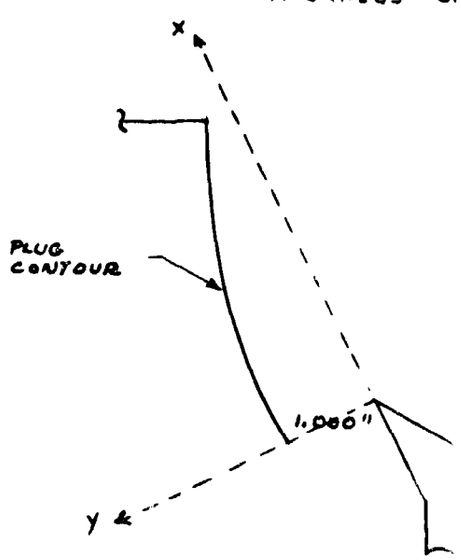

METHOD FOR OBTAINING PLUG CONTOUR

FIG. 34
DIMENSIONS OF TES
APPARATUS

AIR FORCE INSTITUTE W-P AIR FORCE I.
THRUST VECTORING OF PLUG TR
WILLIAM J BARNES JR. 1/LT

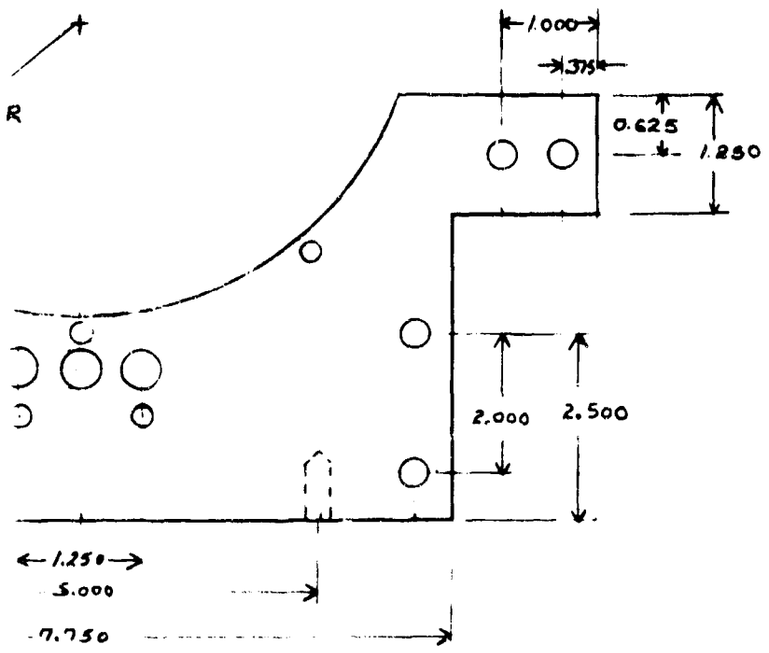

T SIDE PLATE
MAT'L: ALUMINUM

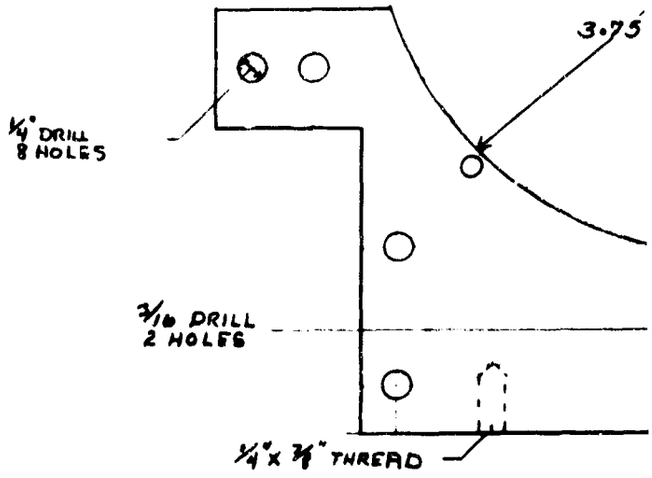

PART NO. 2
THICKNESS = 0.1

PART NO. 4 TRANSLATED
PLUG. THICKNESS = 0.191"
MAT'L: BRASS

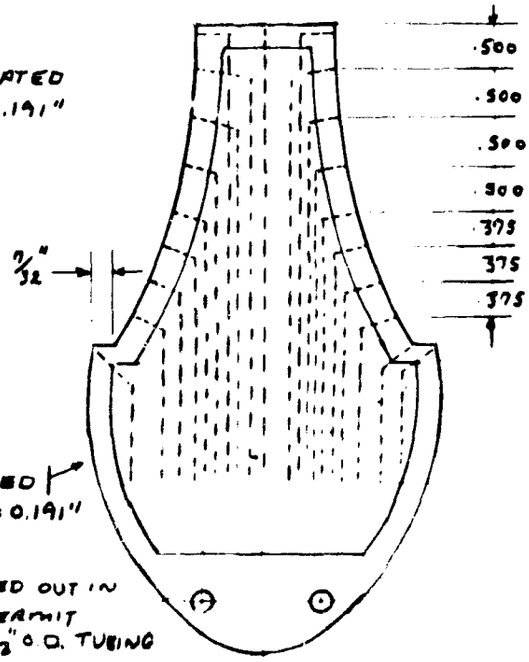

PART NO. 5 CENTERED
PLUG. THICKNESS = 0.191"
MAT'L: BRASS

NOTE: CAVITY MILLED OUT IN FACE OF PLUG TO PERMIT INSTALLATION OF 1/32" O.D. TUBING

NOTE: GLASS RETAINING RINGS NOT SHOWN.

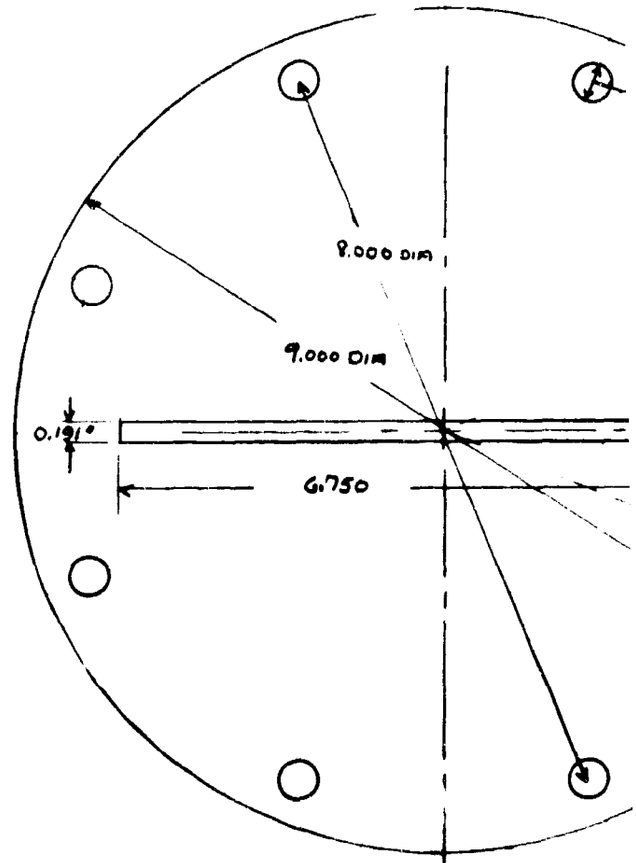

PART NO. 6 BASE PLATE
THICKNESS = 0.500" MAT'L: ALUMIN

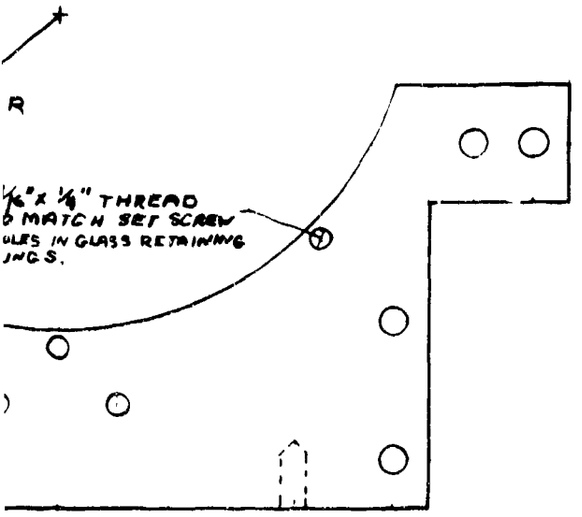

ACK SIDE PLATE
0" MAT'L: ALUMINUM

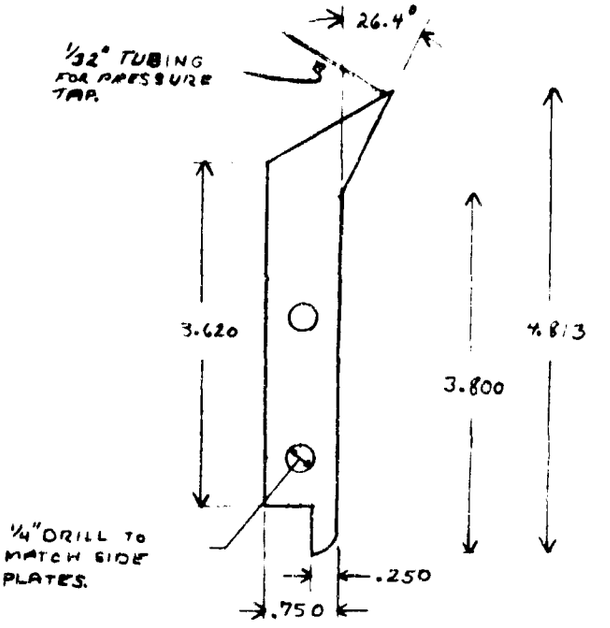

PART NO 3 NOZZLE LIP 2 REQUIRED
THICKNESS = 0.191" MAT'L: BRASS

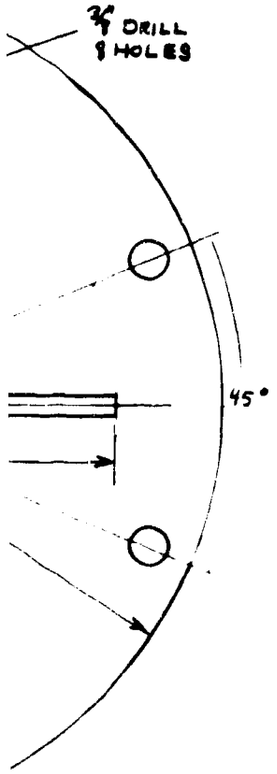

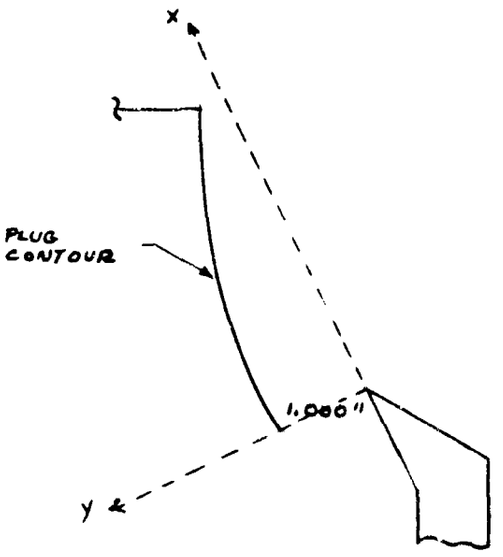

METHOD FOR OBTAINING PLUG CONTOUR

X (IN)	Y (IN)
0.0	1.000
0.329	0.999
0.485	0.997
0.619	0.992
0.746	0.986
0.995	0.965
1.122	0.949
1.235	0.930
1.389	0.907
1.529	0.879
1.676	0.847
1.830	0.808
1.990	0.763
2.162	0.711
2.336	0.651
2.720	0.507
2.925	0.420
3.368	0.213

FIG. 34
DIMENSIONS OF TEST APPARATUS

AIR FORCE INSTITUTE OF TECHNOLOGY
W-P AIR FORCE BASE, OHIO

THRUST VECTORING OF A PLUG NOZZLE BY PLUG TRANSLATION

WILLIAM J BARNES JR. 1/LT GA-64 17 JULY 1964